Meteorological Bulletin

RESEARCH MANUAL 1

ECMWF DATA ASSIMILATION

SCIENTIFIC DOCUMENTATION

ECMWF Research Department

This Meteorological Bulletin is bound separately.

Sheets replaced by updates should be retained at the back of the manual.

2/84 Original Version
10/87 2nd Edition
3/92 3rd Edition

European Centre for Medium-Range Weather Forecasts
Europäisches Zentrum für mittelfristige Wettervorhersage
Centre européen pour les prévisions météorologiques à moyen terme

CONTENTS

CHAPTER 3
Humidity Analysis

CHAPTER 4
Analysis of Surface Fields

CHAPTER 5
Interpolation Methods

CHAPTER 6
Normal Mode Initialization

CONTENTS

CHAPTER 7
Monitoring of Observation and Analysis Quality

CHAPTER 1

Overview

1.1   INTRODUCTION

The main objective of the data assimilation scheme that has been developed   at ECMWF is to provide initial states for the Centre's operational forecast model. The assimilation scheme has also been used to produce analyses from the observations made during the First GARP Global Experiment (FGGE), for use by the international scientific community.   The scheme produces global analyses in numerical form using all appropriate types of available observations.   It is designed to run efficiently, with minimal human intervention, on a large, fast, vector processing computer.

This documentation is designed to cover all scientific aspects of the assimilation. Research and development of the scheme continues, so what is presented in this account is the current status.   Amendments to the documentation will be issued at appropriate intervals.

1.2   DATA ASSIMILATION

An analysis, if it is to be as accurate as possible, must supplement information from the currently available observations by two means:

1.   Information from earlier observations.

2.   Knowledge of the likely structure and scales of atmospheric motion, and of the balance which is usually observed between the various fields (mass, wind, humidity) of the atmosphere.

In a data assimilation scheme both of these are provided with the help of a numerical model of the atmosphere, which can update information from past observations to the current analysis time, and assimilate all the data into a consistent multivariate three dimensional analysis which represents the atmospheric motion in a realistic way.   When, as at ECMWF, the main use of the analysis is to provide initial conditions for a numerical forecast, the advantage of using a numerical model outweighs the main disadvantage, which is that biases and inaccuracies in the model's formulation and limitations to its resolution mean that the final analysis does not always accurately represent all the detail available in the observations.

Ideally, observations should be inserted into the assimilating model at the valid model time. However, this is difficult to organise, particularly if sophisticated analysis methods are used to help ensure that the information is inserted into realistic scales of motion, with approximate balance between the various fields. At ECMWF a compromise 6 hourly intermittent data-assimilation is used, illustrated in Fig. 1.1

Observations from a 6 hour period spanning the nominal analysis time are used to correct a 6 hour forecast made from the previous analysis. Deviations of the observations from the forecast are analysed to give increment fields which are then added to the forecast fields. Details of the mass and wind analysis method are given in Chapter 2. The moisture analysis is described in Chapter 3 and the procedure for updating the surface fields in Chapter 4. The transformations between model and analysis space are described in Chapter 5.

Since the analysis methods cannot represent the atmosphere's balance as accurately as the model can, we use the model equations subsequently in a non-linear normal mode initialisation (Chapter 6). The balance achieved by this is sufficiently realistic that even fields sensitive to the balance, such as the vertical velocity, are meteorologically realistic. For this reason, we usually consider the initialised fields to be the analysis, despite the fact that the uninitialised fields usually fit the individual observations somewhat better.

The initialised analysis is then used as initial conditions for a 9 hour forecast, using the standard version of ECMWF's prediction model. Since we use the forecast field in the next analysis, we also estimate its statistical uncertainty, so it can be given appropriate weight. The methods used for this error estimation are described in Chapters 2 and 3.

A data assimilation scheme can be used to monitor its own performance and observations (Chapter 7).

1.3   ANALYSED VARIABLES AND COORDINATE SYSTEMS

As the main purpose of the analysis is to produce initial conditions for the forecast model, we have chosen the same coordinates in the analysis as in the forecast model currently in use. The analysis system is fully three dimensional as observations are used at their reported 3-D positions. Some observing systems, like radiosondes, measure the atmosphere at a higher vertical resolution than is possible to represent by the analysis or the forecast model. Only a subset of reported levels is selected from such multi-level observations. The selection is defined by 15 standard pressure levels: 1000, 850, 700, 500, 400, 300, 200, 150, 100, 70, 50, 30, 20 and 10 hPa. A data layer is centred at the standard pressure level and its boundaries are halfway between the standard levels. From each layer only one level can be selected, preference being

given to the level closest to a standard pressure level. Thickness and precipitable water observations are given for layers defined by the standard pressure levels.
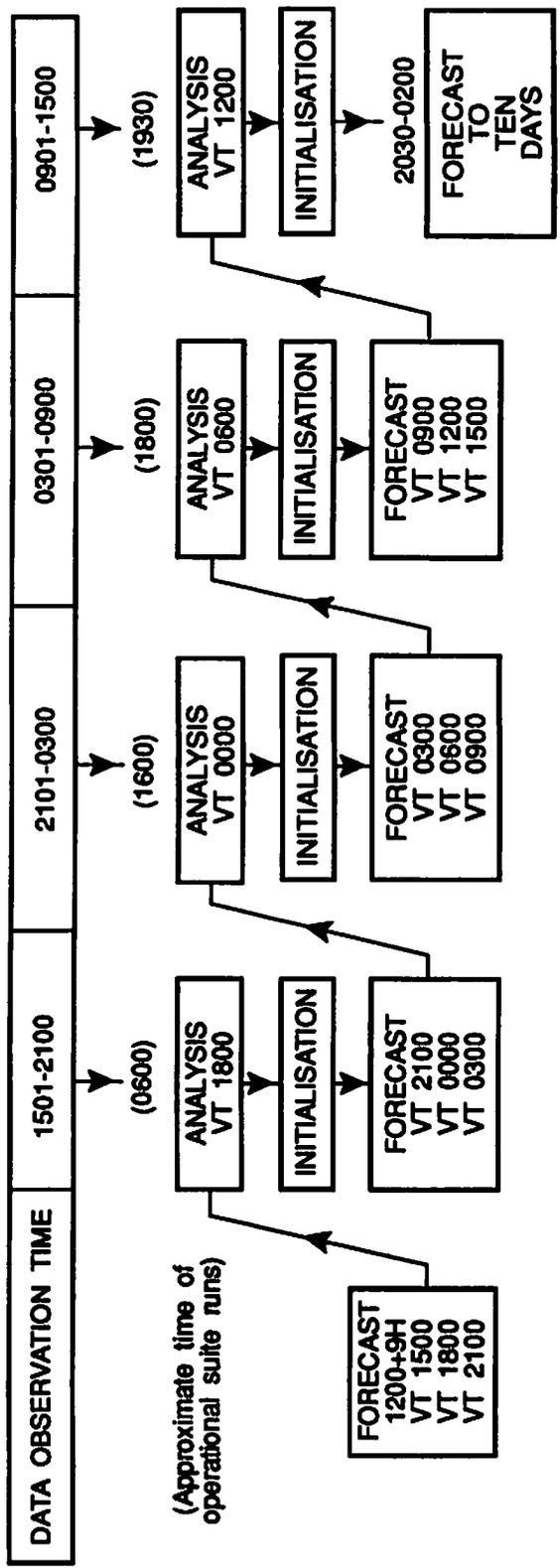
OPERATIONAL DATA ASSIMILATION - FORECAST CYCLE

Fig. 1.1 The 6 hourly intermittent data assimilation.

The analysed variables are geopotential height, and northward and eastward components of wind. Whilst the analysed variable is described as geopotential height, in certain circumstances it is, more precisely, an analysis of geopotential thickness for levels above 150 hPa, in the manner described in Sect. 2.7.4. In addition to geopotential height and wind, a humidity analysis is performed for model levels below 250 hPa. The variable analysed is relative humidity.

1.4   JOB AND FILE STRUCTURE

The three main steps in the data assimilation (analysis, initialisation and forecast) are performed sequentially with files as interfaces where appropriate, as illustrated in Fig. 1.2. Various input and output tasks, which are performed in subsidiary jobs with their own interface files, are shown schematically.

Most analysis functions have been integrated into one job step. The analysis step includes:

- transformation from spectral to grid point space
- estimation of forecast errors from analysis errors of previous cycle
- observation processing
- mass and wind analysis which includes "superobservation" formation, data checking by statistical interpolation and evaluation of analysis increments
- analysis of relative humidity (similar to mass and wind analysis)
- add increments to model first-guess
- transformation from grid point to spectral space.

As part of an assimilation, statistics on the fit of observations to analysis, initialised analysis and first-guess are collected. The data assimilation statistics also include quality control flags.
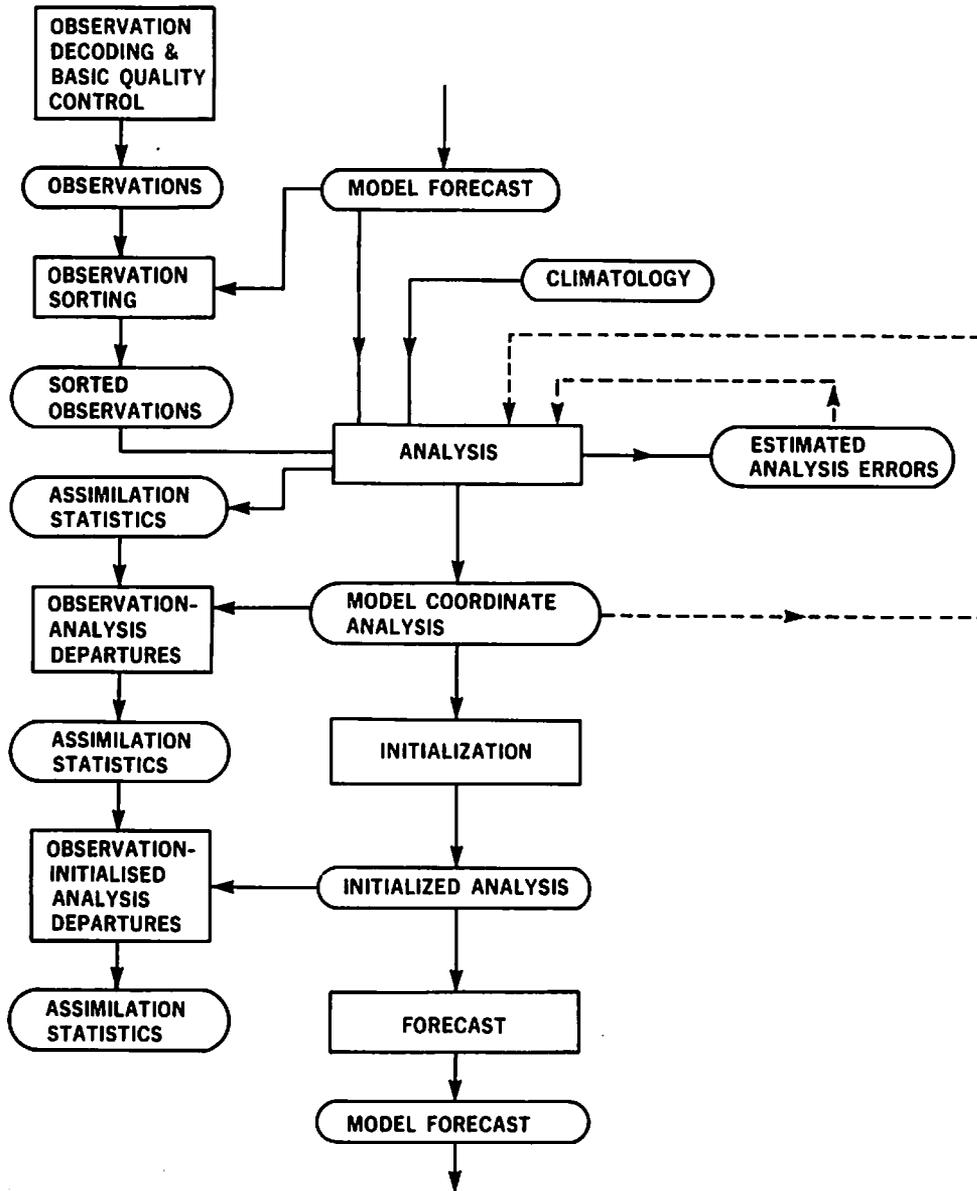
Fig. 1.2 Job and file structure of an assimilation cycle.

CHAPTER 2

Mass and Wind Analysis

2.1   INTRODUCTION

The analysis method is an extension of optimal interpolation (*Eliassen*, 1954 and *Gandin*, 1963) to a multivariate three-dimensional interpolation of deviations of observations from a forecast field (*Lorenc*, 1981). This technique allows consistent use to be made of observations with different error characteristics, and takes into account their spatial distribution. The equations are set out in Section 2.2. Because of the various assumptions made in using linear regression and error covariance modelling the interpolation is not truly optimal and the name 'statistical interpolation' is preferred. The abbreviation OI will be frequently used.

Linear relationships can be specified in a statistical interpolation scheme between meteorological variables that are analysed simultaneously.

Schlatter (1975) and *Rutherford* (1976) have used the geostrophic relationship in this way, *Rutherford* (1976) the hydrostatic, and *Schlatter et al.* (1976) the (non-divergent) streamfunction-wind relationship. The relationships used in the ECMWF scheme are described fully in Section 2.3. Their use causes the analysed corrections to the forecast to be locally approximately non-divergent and approximately geostrophic, with the geostrophic relationship relaxed near the equator. The hydrostatic relationship enters only in the conversion of temperature observations to thicknesses.

The analysis variables and the horizontal and vertical coordinates were described in Section 1.3. Input to the analysis consists of observed minus forecast values of the same variables. The processing of the various types of observations to give information for these variables is described in Section 2.4.

The scheme has been designed for a vector processing computer especially suitable for the efficient solution of large linear systems of equations. In contrast, the logical operations usually required for selecting only the 'best' data in order to keep the systems small do not exploit the full speed of a vector processing machine. Thus instead of the small systems, typically of order 10 to 50, used in other schemes, the ECMWF scheme uses large systems of order 200 or more. This also enables the full potential of the multivariate three-dimensional statistical analysis method to be exploited, since within such a large number of data it is possible to include height, wind and thickness data for several layers of the atmosphere. For example only by three-dimensional use of the data can optimum use be made of a surface pressure observation, a set of satellite temperature soundings, and a cloud motion wind. The thickness and thickness gradient (thermal wind) information in the soundings increases the "zone of influence" of the pressure and wind data. It is

neither necessary nor practicable to select data, or solve large systems of equations, for each analysis grid point and variable. Instead this is done for volumes containing several gridpoints and levels.

In this documentation we frequently use the concepts "model box" and "analysis box". The corners of a model box are defined by adjacent points, in zonal and meridional direction, of the forecast model's Gaussian grid. Much of the analysis calculation are done on batches of observations, not single reports. The area or volume which contains such a group of data is called an "analysis box" or "analysis volume". The definition is vaguer than that of the "model box". We associate with an "analysis box" such concepts as analysis overlap boundaries, minimum and maximum data selection boundaries. Preciser definitions are given in the data selection part. To control the handling of analysis volumes an information tree or "box" tree is constructed. This tree contains in addition to information on boundaries also links to allow sequential processing of the "analysis boxes". The tree is dynamic as it depends on data density and the analysis mode (data checking, analysis evaluation for either mass and wind or humidity analysis).

Several tests are applied to the data to identify and exclude erroneous observations from the data set that is used for the analysis. Section 2.5 describes the test against the first-guess and the full multivariate check by the OI equations. The mathematical formulae of the OI data check are derived in Section 2.2.3.

The selection of the data used for the analysis of each analysis volume is described in detail in Section 2.6. The criteria used are generally based on assessments of local data amounts, rather than evaluation of the usefulness of any one datum. Within each model box, if there is a surfeit of data, close observations of the same type which agree with each other are combined to form 'super-observations'. The observations which contributed to the 'super-observations' have no further use in the analysis. Similarly, stations that reported more than once during the six hour period provide only one observation for the analysis calculations. At the end of the observation processing a compressed array of non-redundant observations is constructed for the following steps of the analysis.

The next step is quality control of the remaining data by statistical interpolation. For this step a box tree is constructed according to the data selection parameters of quality control (QC). All data presented to the QC step are checked against an independent analysis using neighbouring data.

The QC is followed by the evaluation of increments using only those data which passed the QC. A new box tree with another set of selection parameters is set up to control the evaluation. The analysis of relative humidity is done in the same way; QC and analysis evaluation including the construction of box trees.

The computational organisation of the mass and wind analysis is explained in Section 2.7.
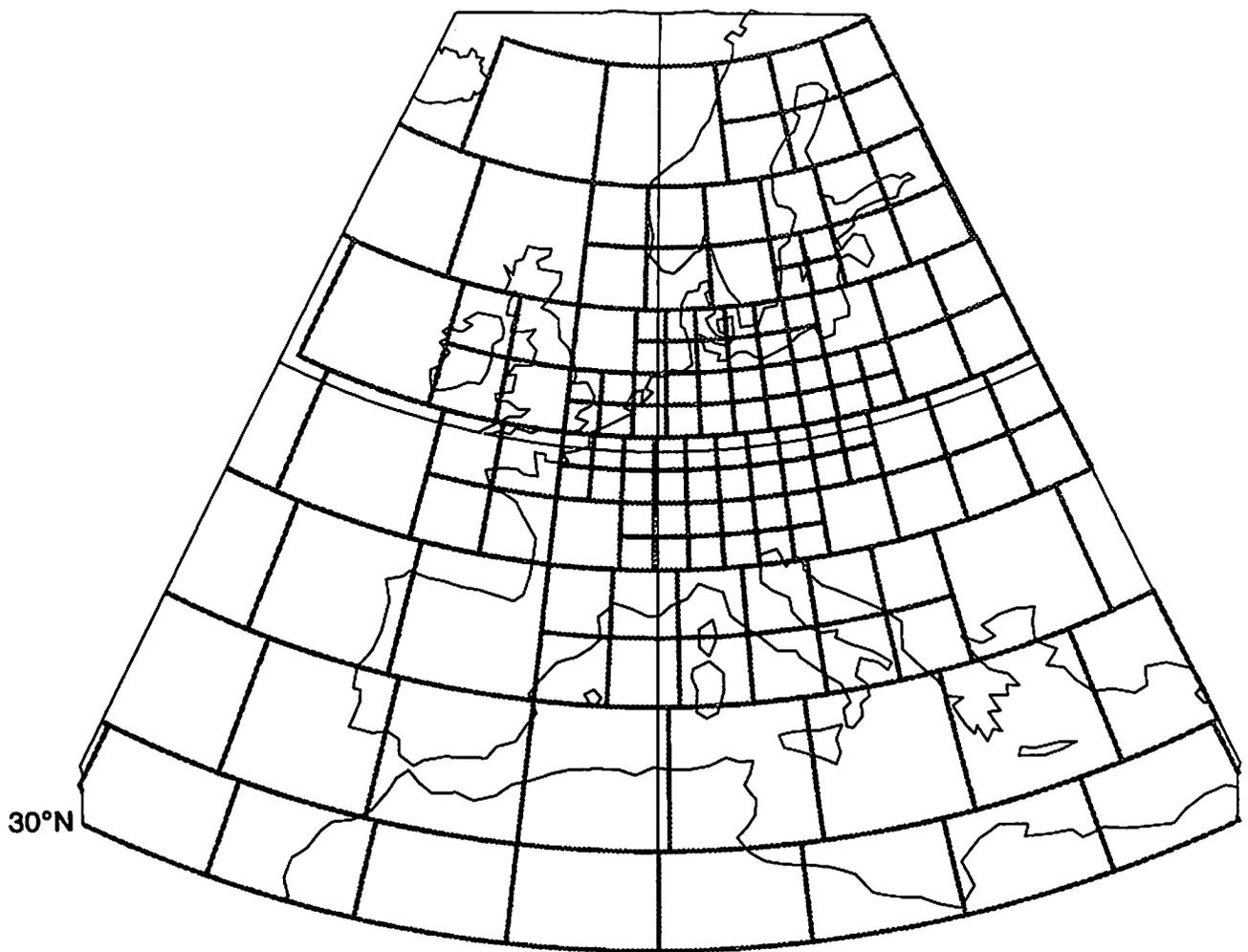
Fig. 2.1 Analysis box structure.

30°N

2.2 DESCRIPTION OF METHOD

Three different applications of the well known statistical (optimal) interpolation technique are used in the scheme: to form 'super-observations', to check data, and to produce grid point values while excluding rejected data (without repeating the solution of the large linear system). It is convenient to include the derivation of the three sets of equations in this section together with a derivation of the basic statistical interpolation equations.

2.2.1 Statistical interpolation

The basic technique used is a three-dimensional, multivariate, statistical interpolation of normalised deviations from a predicted field, where the normalisation factors are the estimated root mean square errors of the predicted values.

Using A to represent any scalar variable, and E to represent its estimated rms error, with superscripts i, p, o and t respectively denoting interpolated, predicted, observed and true value, the basic interpolation equation is thus

$$\frac{A_k^i - A_k^p}{E_k^p} = \sum_{n=1}^{N} w_{kn} \frac{A_n^o - A_n^p}{E_n^p} \tag{2.2.1}$$

where subscript k denotes the point and variable being analysed and subscripts $n = 1,N$ range over all points and variables of observations selected for the analysis of variable and position k.

Next, we want to determine the weights w_{kn} to be given each observation in such a way that we minimise the analysis error over an ensemble of similar realisations.

Writing

$$\alpha_n^o = \left(A_n^o - A_n^t \right) / E_n^o$$

$$\alpha_n^p = \left(A_n^p - A_n^t \right) / E_n^p$$

$$\alpha_k^i = \left(A_k^i - A_k^t \right) / E_k^i$$

$$e_n^o = E_n^o / E_n^p$$

$$e_k^i = E_k^i / E_k^p$$

equation (2.2.1) becomes

$$\alpha_k^i e_k^i = \alpha_k^p + \sum_{n=1}^{N} w_{kn} \left(\alpha_n^o e_n^o - \alpha_n^p \right) \tag{2.2.2}$$

Squaring (2.2.2), and taking the ensemble average (denoted by $< \, , \, >$) over several similar situations gives

$$e_k^{\prime 2} = 1 + 2 \sum_{n=1}^{N} w_{kn} \left(<\alpha_k^p \, , \, \alpha_n^o> e_n^o - <\alpha_k^p \, , \, \alpha_n^p> \right)$$

$$+ \sum_{m=1}^{N} \sum_{n=1}^{N} w_{km} \left(<\alpha_m^p, \alpha_n^p> + e_m^o <\alpha_m^o, \alpha_n^o> e_n^o - e_m^o <\alpha_m^o, \alpha_n^p> - <\alpha_m^p, \alpha_n^o> e_n^o \right) w_{kn} \qquad (2.2.3)$$

To simplify subsequent algebra we assume at this point that the correlations of prediction and observation errors are zero, i.e.

$$<\alpha_m^o, \alpha_n^p> = <\alpha_m^p, \alpha_n^o> = 0$$

This assumption is reasonable for the types of observation currently available; if necessary it could be relaxed. We also introduce a vector and matrix notation:

$\underline{W}_k$ is the column vector of weights w_{kn}

$\underline{P}$ is the prediction error correlation matrix $\left[<\alpha_m^p, \alpha_n^p> \right]$

$\underline{Q}$ is the scaled observation error correlation matrix $\left[e_m^o <\alpha_m^o, \alpha_n^o> e_n^o \right]$

$\underline{M} = \underline{P} + \underline{Q}$

$\underline{B}$ is the vector of normalised increments $\dfrac{A_n^o - A_n^p}{E_n^p}$

$\underline{P}_k$ is the vector of prediction error correlations $<\alpha_k^p, \alpha_n^p>$

Equation (2.2.3) becomes

$$e_k^{\prime 2} = 1 - 2 \underline{w}_k^T \underline{P}_k + \underline{W}_k^T \underline{M} \, \underline{W}_k \qquad (2.2.4)$$

The 'optimal' weight vector is that which minimises the estimated normalised interpolation error variance $e_k^{\prime 2}$. By equating $\dfrac{\partial e_k^{\prime 2}}{\partial w_{kn}}$ to zero for n = 1, N we get a set of linear equations for the optimal weights:

$$\underline{W}_k = \underline{M}^{-1} \underline{P}_k \qquad (2.2.5)$$

The minimum value of $e_k^{\prime 2}$ corresponding to these weights is given by

$$e_k^{\prime 2} = 1 - \underline{W}_k^T \underline{P}_k \qquad (2.2.6)$$

This expression gives the correct value of the analysis error only when the statistics used in the OI scheme are exactly known. For the data checking and the estimation of the subsequent six hour forecast error, a more realistic estimate than that given by (2.2.6) is needed. Such an estimate is obtained by inflating (2.2.6) for uncertainties in the statistics and for errors in scales not resolved by the analysis (see Section 2.5.3(g)).

The optimal interpolation equation for the normalised deviation from the predicted field is thus:

$$\frac{A_k^i - A_k^p}{E_k^p} = B^T \underline{W}_k \qquad (2.2.7)$$

If interpolated values are required for several points and variables A_k, it is convenient to eliminate $\underline{W}_k$ from (2.2.5) and (2.2.7):

$$\frac{A_k^i - A_k^p}{E_k^p} = B^T \underline{M}^{-1} \underline{P}_k \qquad (2.2.8)$$

Since $\underline{M}^{-1}$ and B are independent of the point being analysed, their product needs to be evaluated only once to give a vector of coefficients $\underline{C}$.

$$\frac{A_k^i - A_k^p}{E_k^p} = \underline{C}^T \underline{P}_k \qquad (2.2.9)$$

2.2.2   Super-observation formation

This section deals only with the mathematical limitations imposed by OI in forming averaged observations. The practical aspects of "super-observation" creation are described in Section 2.6.2(b). If the standard optimal interpolation technique were used to create the super-observation then the interpolated value would contain information from, and hence be correlated with, the predicted value A_k^p. This is inconvenient since for ordinary observations it is assumed that $<\alpha_m^p, \alpha_n^o> = 0$. Consequently the interpolation equations used for super-observation formation are modified by imposing a constraint that no information is taken from the local predicted value. Using the notation $^\wedge$ to indicate those values which differ in the modified method, the constraint can be expressed:

$$<\hat{\alpha}_k^i, \alpha_k^p> = 0 \qquad (2.2.10)$$

Using (2.2.2) to expand this, and using vector notation gives

$$\hat{\underline{W}}_k^T \underline{P}_k = 1 \qquad (2.2.11)$$

The interpolation error is still given by (2.2.4)

$$\hat{e}_k^{i^2} = 1 - 2\hat{W}_k^T P_k + \hat{W}_k^T \underline{M} \hat{W}_k \qquad (2.2.12)$$

Minimising this with the constraint (2.2.11) gives the following equation for the constrained weights

$$\hat{W}_k = (1 + \lambda) \underline{M}^{-1} P_k \qquad (2.2.13)$$

Comparing this with (2.2.5) we see that the constraint forces a renormalisation of the interpolation weights:

$$\hat{W}_k = (1 + \lambda) W_k \qquad (2.2.14)$$

with λ defined by substitution back in (2.2.11)

The error in the interpolated super-observation is given by substituting (2.2.11) and (2.2.13) in (2.2.12):

$$\hat{e}_k^{i^2} = \lambda \qquad (2.2.15)$$

Super-observation formation is restricted in the ECMWF system to close observations of the same type and within the same model box. The averaging is preceded by a full quality control by statistical interpolation using observations of the same type from the model box itself and neighbouring boxes.

2.2.3 Observation checking

When checking a datum k we compare its normalised deviation from the predicted value $\left(A_k^o - A_{k_p}\right)/E_k^p$ with

an interpolated deviation using nearby data $\left(A_k^i - A_k^p\right)/E_k^p$. Hence it is appropriate when deriving the

equations for this interpolation to minimise the expected variance of the difference between the two

deviations, rather than the deviation from the true value. Thus instead of (2.2.4) we minimise:

$$e_k^{i^2} = e_k^{o^2} + 1 - 2W_k^T M_k + W_k^T \underline{M} W_k \qquad (2.2.16)$$

If the datum being checked is also used for the interpolation then M_k is a column of $\underline{M}$ and minimising

(2.2.16) leads to the trivial result

$$W_k = D_k \qquad (2.2.17)$$

where D_k is defined as a vector whose k'th element is unity and other elements are zero, i.e. since we are

trying to interpolate a value for the observation including its observation error, the best estimate is naturally

the observation itself. What we must do is minimise (2.2.16) subject to the strong constraint that certain data

(datum k and perhaps others) are given zero weight. Using $^\wedge$ to indicate values obtained with the

constraints, the constraints can be expressed:

$$D_{1(l)}^T \hat{W}_k = 0 \quad (1 = 1, n \text{ constraints}) \qquad (2.2.18)$$

Minimising (2.2.16) with these constraints gives

$$\hat{W}_k = W_k + \sum_{i=1}^{n\ constr.} \lambda_i \underline{M}^{-1} D_{1(i)} \tag{2.2.19}$$

The multipliers λ_i can be found by multiplying by $D_{1(i)}^T$ and using (2.2.18)

$$\sum_{i=1}^{n\ constr.} D_{1(i)}^T \underline{M}^{-1} D_{1(i)} \lambda_i = -D_{1(i)}^T W_k \quad \text{for } j = 1, n \text{ constraints}) \tag{2.2.20}$$

Substituting (2.2.18) and (2.2.19) back in (2.2.16) gives:

$$e_k^{\hat{o}^2} = e_k^{o^2} + 1 - \hat{W}_k^T M_k \tag{2.2.21}$$

2.2.4 Grid point analysis

The matrix inverse $\underline{M}^{-1}$ used in the data checking equations is expensive to compute, so it can be advantageous to re-use it when performing the grid-point analysis rather than computing a slightly different one. This optional feature of the analysis scheme is currently not used as the required storage space for the matrices exceeds the available disk space. Rather than reinverting the correlation matrix, a linear system of equations is solved. However, for completeness both methods are described in the following.

2.2.4(a) Grid point analysis by re-use of matrix inverse

The inverted matrices include data which have been rejected during the checking phase, and it is therefore necessary to apply constraints that these rejected data are given zero weight. Thus we need to minimise (2.2.4) with constraints like (2.2.18). Again using ^ to indicate values obtained with the constraints, we get:

$$\hat{e}_k^{\hat{i}^2} = 1 - 2 \hat{W}_k^T P_k + \hat{W}_k^T \underline{M} \hat{W}_k \tag{2.2.22}$$

$$D_{1(i)}^T \hat{W}_k = 0 \quad (i = 1, n \text{ constraints}) \tag{2.2.23}$$

This gives:

$$\hat{W}_k = W_k + \sum_{i=1}^{n\ constr.} \lambda_i \underline{M}^{-1} D_{1(i)} \tag{2.2.24}$$

The multipliers λ_i can be found as in (2.2.20):

$$\sum_{i=1}^{n\ constr.} D_{1(i)}^T \underline{M}^{-1} D_{1(i)} \lambda_i = -D_{1(i)}^T W_k \quad (\text{for } j = 1, n \text{ constraints}) \tag{2.2.25}$$

The interpolation error is given by

$$e_k^{'2} = 1 - \hat{W}_k^T P_k \tag{2.2.26}$$

In order to derive an equation similar to (2.2.9) it is convenient to extend the matrix notation. We define a vector λ of the Lagrangian multipliers λ_l, and a rectangular matrix E having its l 'th column equal to $D_{l(i)}$. The summation in (2.2.24) can then be expressed in matrix terms:

$$\hat{W}_k = W_k + \underline{M}^{-1} \underline{E} \lambda \tag{2.2.27}$$

The vector λ is the solution of (2.2.25)

$$\underline{E}^T \underline{M}^{-1} \underline{E}\lambda = -\underline{E}^T W_k \tag{2.2.28}$$

Substituting (2.2.28) in (2.2.27) gives:

$$\hat{W}_k = W_k - \underline{M}^{-1} \underline{E} \left(\underline{E}^T \underline{M}^{-1} \underline{E}\right)^{-1} \underline{E}^T W_k \tag{2.2.29}$$

Substituting (2.2.29) in (2.2.27) gives the equivalent equations for (2.2.28) and (2.2.29).

$$\frac{A_k^i - A_k^p}{E_k^p} = \left(\left(B^T \underline{M}^{-1}\right) - \left(B^T \underline{M}^{-1}\right) \underline{E} \left(\underline{E}^T \underline{M}^{-1}\underline{E}\right)^{-1} \underline{E}^T \underline{M}^{-1}\right) P_k \tag{2.2.30}$$

$$= \underline{C}^T P_k \tag{2.2.31}$$

Brackets indicate the most efficient order of computation, remembering that $\underline{E}$ has only a few columns (~5 perhaps) and ~150 rows at present. Multiplication by $\underline{E}$ is not implemented as a matrix operation; $\underline{E}$ is not stored as such, only $D_{l(i)}$. Multiplication by $\underline{E}$ is equivalent to looking up elements $D_{l(i)}$ in the multiplicand.

All vectors except P_k are independent of the grid point being analysed and hence the rest of the calculation (to find the analysis coefficients vector $\underline{C}$) can be done outside of the loop over grid points.

The analysis error is given by substitution in (2.2.26)

$$e_k^{'2} = 1 - P_k^T \left(\underline{M}^{-1} P_k\right) + \left(P_k^T \underline{M}^{-1}\right) \underline{E} \left(\underline{E}^T \underline{M}^{-1} \underline{E}\right)^{-1} \left(\underline{E}^T \underline{M}^{-1}\right) P_k \tag{2.2.32}$$

The evaluation of this requires a matrix multiplication $\underline{M}^{-1}P_k$ per grid point.

The method used to calculate the inverse is Cholesky decomposition. The symmetric positive definitive matrix $\underline{M}$ is decomposed to a form $\underline{M} = \underline{LDL}^T$, where $\underline{L}$ is a lower triangular matrix and $\underline{D}$ a diagonal matrix. The inverse is then solved from $\underline{M}^{-1} = (\underline{L}^T)^{-1} \underline{D}^{-1} \underline{L}^{-1}$.

The matrix $\underline{M}$ is regarded as ill-conditioned if

$$\underset{\substack{i=1,n \\ j=1,n}}{Max} \ |\frac{1}{b_{ij}}| \ \leq \ \frac{2n^4 p}{\gamma}$$

where n is the order of the matrix, p is the machine precision (2^{-48}), γ the relative accuracy which is demanded of the solution and b_{ij} are the elements of the inverse of $\underline{M}$ (*Hollingsworth and Cats*, 1985). To reduce the possibility of ill-conditioning, the normalised observation error is set to 0.5 if the ratio between observation and forecast error is less than 0.5.

2.2.4(b) Grid point analysis by solution of a linear system

Evaluation of the interpolated values in (2.2.9) requires the computation of the coefficient vector $\underline{C} = \underline{M}^{-1} \underline{B}$.

Instead of calculating the inverse of $\underline{M}$, $\underline{C}$ is solved from

$$\underline{M} \ \underline{C} = \underline{B} \tag{2.2.33}$$

by Gaussian triangularisation and elimination.

When solving the linear system of equations, no condition number can be calculated. According to *Cats* (1981) all diagonal elements of the matrix should exceed:

$$c > 1 + \frac{pn^{3.5}}{E(1-K)} \tag{2.2.34}$$

where

    c = diagonal element

    p = relative machine precision

    E = desired accuracy (10^{-4})

    K = maximum observation error correlation

    n = order of matrix

The condition imposed in the analysis code is

$$c > 1 + \frac{pn^{3.5}}{E} + K(c-1)$$

(2.2.35)

2.3   FIRST-GUESS ERROR STATISTICS

2.3.1   General considerations

To solve the analysis equations we need values for the expected first-guess error covariances between all variables and positions which are analysed or which have useful observations. Even if empirical data for these were available, it would be impossible to tabulate them for every possible combination, so they must be modelled. The first-guess is usually a forecast, although it can be a climatological mean, persistence, or some combination of these. Its error is the difference between this predicted value and the "true" value. The "true" is in quotes since we exclude from it scales of motion smaller than those we wish to analyse. For the rest of Section 2.3, unless explicitly stated otherwise, equations, errors and correlations refer to such prediction errors.

Relationships assumed while modelling the error covariance can have a direct effect on the properties of the analysis increments. For example covariances of the thickness Δh_{12} are calculated from those of the heights using the equation $\Delta h_{12} = h_2 - h_1$. This means that as long as the same data are used for each, the analysed increments to the predicted field will obey the same equation, even if there are data for the three variables which do not obey it. Thus our choice of covariance model is governed by the relationships which we wish the analysed increments to obey, as well as by the available empirical data and convenience of use.

In the mass and wind analysis the data used are geopotential heights and winds at a set of pressure levels, and geopotential thicknesses between the levels. Relevant observations of other variables, for example sea level pressure, are converted to these input variables before use.

The analysed variables are height and wind on model levels. Thus covariances are needed between all of these. The computation is so organised that it is convenient to specify each covariance as the product of the appropriate errors and a correlation. Continuous functional representations are used for both horizontal and vertical correlations. We assume that correlations between points at different levels and horizontal positions can be expressed as a product of the corresponding vertical and horizontal correlations. Details are given in Sects. 2.3.2 to 2.3.7.

2.3.2 Height error model

As explained in Section 2.3.1 the errors and correlations for the different variables need to obey certain relationships if we wish the analysis increments also to obey them. This is easiest to ensure if we first specify the geopotential height errors and their correlations and then specify compatible models for the other variables.

Height errors (E_h) are specified as a smooth global three dimensional field. Their correlations are specified as the product of a vertical correlation function (M_h) which varies only slowly with horizontal position, and a horizontal function (F_h) whose scale length L varies slowly with horizontal position. The horizontal model used is a series of Bessel functions of the distance between the points correlated (r_{ij}):

$$F_h\left(r_{ij}\right) = \sum_{n=0}^{8} A_n \, J_0\left(k_n \, r_{ij} / D\right)$$
(2.3.1)

The wavenumbers k_n are specified by zero derivative boundary conditions at $r=D$. J_0 is the Bessel function of the first kind and zero order, and A_n is the amplitude of radial mode n. The scale of the correlation function F is defined as

$$L_F^2 = -\left(\frac{F}{\nabla^2 F}\right)_{r=0}$$

Substitution of (2.3.1) into the above definition gives

$$L_F^2 = D^2 \, \frac{\sum A_n}{\sum k_n^2 A_n}$$

The numerical values of the scale length are given in Section 2.3.5(a).

For each radial mode it has been possible to determine the vertical correlation from observations (*Hollingsworth and Lönnberg*, 1986 and *Lönnberg and Hollingsworth*, 1986). The data studies show a strong dependence of the scale height on horizontal mode. Consequently, we have introduced the following 3-dimensional correlation model for height:

$$F = A_o \, M_{LS} + \sum_{n=1}^{8} A_n \, J_0\left(k_n \, r/D\right) M_{SYN}$$

where M_{LS} is the vertical correlation of the large scale, horizontally constant, mode. M_{SYN} is the vertical correlation of the radially varying modes (synoptic scales).

The same shape of the correlation function is used globally, i.e. the amplitudes A_i do not vary with geographical location. The values A_i are as follows:

$A_0 = 0.15$	$A_3 = 0.14$	$A_6 = 0.03$
$A_1 = 0.30$	$A_4 = 0.08$	$A_7 = 0.02$
$A_2 = 0.28$	$A_5 = 0.05$	$A_8 = 0.01$

As the evaluation of Bessel functions is very costly, the series (2.3.1) and its first and second derivatives are approximated by Chebyshev polynomials. For the details of this approximation see Section 2.3.7.

2.3.3 Thickness error model

Once the height errors and correlations are defined everywhere we have no freedom for those for thickness since the equation $\Delta h_{12} = h_2 - h_1$ must be obeyed. Thus the covariance between the thickness and any other variable can be calculated from the height covariances:

$$<a,\Delta h_{12}> = <a,h_2> - <a,h_1> \qquad (2.3.2)$$

Note that since this equation relates the covariances the thickness errors and correlations each depend on both the height errors and the height correlations.

2.3.4 Wind error model

The modelling of wind errors and correlations is the most difficult, since it is a vector quantity and since the relationships which we wish the analysed increments to obey are only approximate. The first problem is overcome by modelling the streamfunction and velocity potential errors, and deriving those for the horizontal wind components by differentiation. The streamfunction error covariances are expressed in a similar way to those of the height errors, as a product of the prediction errors (E_ψ) specified as a smooth global three-dimensional field, a vertical correlation function (M_ψ), and a horizontal correlation function (F_ψ). As with the height model the horizontal variation of E_ψ and M_ψ and the horizontal and vertical variation of the coefficients of F_ψ are assumed to be slow. Thus a general streamfunction - streamfunction covariance is

$$<\psi_i , \psi_j> = E_{\psi_i} E_{\psi_j} M_{\psi_{ij}} \Gamma^2 F_\psi (r_{ij}) \quad \text{where} \quad F_\psi(\eta) = \sum_{n=0}^{8} A_n J_0 (k_n r_{ij}/D) \qquad (2.3.3)$$

$$E_\psi^2 = \lim_{r_{ij} \to 0} <\psi_i, \psi_j> = E_\psi^2 \Gamma^2 \sum_{n=0}^{8} A_n \quad \text{and} \quad \Gamma^2 = \frac{1}{\sum_{n=0}^{8} A_n}$$

$$<\psi_i, \psi_j> = E_{\psi_i} E_{\psi_j} M_{\psi_{ij}} \frac{1}{\sum_{n=0}^{8} A_n} F_\psi(r_{ij}) \qquad (2.3.4)$$

For the divergent part of the wind field error a velocity potential covariance is defined (see *Daley*, 1985 and *Undén*, 1989)

$$<\chi_i\ \chi_j> \ -\ E_{\chi_i}E_{\chi_j}M_{\chi_{ij}}\Omega^2 F_\chi(r_{ij}) \quad \text{and} \quad F_\chi\ -\ F_\psi \quad \text{from (2.3.3)}$$

$$E_\chi^2\ -\ \lim_{r_{ij}\to 0}\ <\chi_i\ \chi_j>\ -\ E_\chi^2\ \Omega^2\ \sum_{n=0}^{8} A_n \quad \text{and} \quad \Omega^2\ -\ \frac{1}{\sum_{n=0}^{8} A_n}$$

$$<\chi_i\ \chi_j>\ -\ E_{\chi_i}E_{\chi_j}M_{\chi_{ij}}\ \frac{1}{\sum_{n=0}^{8} A_n}\ F(r_{ij}) \qquad (2.3.5)$$

The velocity potential horizontal structure F_χ has been chosen to be the same as for the streamfunction (F_ψ). Cross-covariances between streamfunction and velocity potential, as well as between velocity potential and geopotential, have been set to zero.

The total wind prediction error variance E_{v2} is divided into a divergent part (v) and a non-divergence part $(1-v)$

$$E_{v2}\ -\ Ev_\psi^2\ +\ Ev_\chi^2 \qquad (2.3.6)$$

$$Ev_\chi^2\ -\ vE_{v2} \qquad (2.3.7)$$

$$Ev_\psi^2\ -\ (1-v)\ E_{v2} \qquad (2.3.8)$$

The velocity field can be expressed in terms of horizontal derivatives of the streamfunction and velocity potential. From Helmholtz's theorem:

$$v\ -\ \nabla\chi\ +\ k\ \times\ \nabla\psi \qquad (2.3.9)$$

Covariances between wind components can then be expressed in terms of derivatives of streamfunction and velocity potential correlations assuming there is locally no horizontal variation in the error variances. Natural co-ordinates are employed where the longitudinal axis is along the line connecting the two points (i and j) and the transverse axis is perpendicular to that line. u^l is the longitudinal horizontal velocity component and u^t is the transverse component. If we ignore horizontal derivatives of E_ψ, E_χ, M_ψ, M_χ and of the coefficients in F they can be written as (see e.g. *Hollingsworth and Lönnberg*, 1986)

$$<u_i' \, u_j'> = -M_{\psi_{ij}} \frac{1}{r_{ij}} \frac{\partial}{\partial r_{ij}} <\psi_i \, \psi_j> - M_{\chi_{ij}} \frac{\partial^2}{\partial r_{ij}^2} <\chi_i \, \chi_j> \qquad (2.3.10)$$

$$<u_i' \, u_j'> = -M_{\psi_{ij}} \frac{\partial^2}{\partial r_{ij}} <\psi_i \, \psi_j> - M_{\chi_{ij}} \frac{1}{r_{ij}} \frac{\partial}{\partial r_{ij}} <\chi_i \, \chi_j> \qquad (2.3.11)$$

$$<u_i' \, u_j'> - <u_i' \, u_j'> = 0$$

The derivatives of the horizontal correlation function (2.3.3) are:

$$\frac{\partial F}{\partial r_{ij}} = -\sum_{n=1}^{8} A_n \left(\frac{k_n}{D}\right) J_1 \left(\frac{k_n}{D} r_{ij}\right) \qquad (2.3.12)$$

$$\frac{\partial^2 F}{\partial r_{ij}^2} = -\sum_{n=1}^{8} A_n \left(\frac{k_n}{D}\right)^2 J_0 \left(\frac{k_n}{D} r_{ij}\right) + \frac{1}{r_{ij}} \sum_{n=1}^{8} A_n \left(\frac{k_n}{D}\right) J_1 \left(\frac{k_n}{D} r_{ij}\right) \qquad (2.3.13)$$

The wind vector variance can be expressed in terms of streamfunction and velocity potential variances from (2.3.10 and 11) and from (2.3.4 and 5)

$$E_{v^2} = E_{u_i^2}^2 + E_{u_i^2}^2 = \lim_{r_{ij} \to 0} \left(<u_i' \, u_j'> + <u_i' \, u_j'> \right)$$

$$E_{v^2} = \frac{\sum\limits_{n=1}^{8} A_n \left(\frac{k_n}{D}\right)^2}{\sum\limits_{n=0}^{8} A_n} \left(E_\psi^2 + E_\chi^2 \right) \qquad (2.3.14)$$

and the streamfunction and velocity potential variance can be written in terms of the total wind vector variance using the definitions (2.3.7 and 8) as:

$$E_\psi^2 = (1-\nu) \frac{\sum\limits_{n=0}^{8} A_n}{\sum\limits_{n=1}^{8} A_n \left(\frac{k_n}{D}\right)^2} E_{v^2} \qquad (2.3.15)$$

$$E_\chi^2 = \nu \frac{\sum\limits_{n=0}^{8} A_n}{\sum\limits_{n=1}^{8} A_n \left(\frac{k_n}{D}\right)^2} E_{v^2} \qquad (2.3.16)$$

The wind component variances are related to the vector variance by

$$E_{u_i}^2 - E_{u_i}^2 - 1/2 \, E_{v^2}$$

(2.3.17)

due to isotropy.

The wind component correlations then follow from (2.3.10), (2.3.11) and (2.3.17)

$$corr\!\left(u_i^l \, u_j^l\right) = \frac{<u_i^l \, u_j^l>}{Eu_i^l \, Eu_j^l} = 2 \, \frac{<u_i^l \, u_j^l>}{Ev_i \, Ev_j}$$

$$corr\!\left(u_i^l \, u_j^l\right) = -M_{\psi\psi} \, \frac{E_{\psi i} \, E_{\psi j}}{\displaystyle\sum_{n=0}^{8} A_n} \, \frac{2}{Ev_i \, Ev_j} \, \frac{1}{r_{ij}} \, \frac{\partial}{\partial r_{ij}} \, F(r_{ij})$$

$$-M\chi \, \frac{E\chi_i \, E\chi_j}{\displaystyle\sum_{n=0}^{8} A_n} \, \frac{2}{Ev_i \, Ev_j} \, \frac{\partial^2}{\partial r_{ij}} \, F(r_{ij})$$

and using the results from (2.3.15 and 16)

$$corr\!\left(u_i^l \, u_j^l\right) = - \frac{2(1-\nu)}{\displaystyle\sum_{n=0}^{8} A_n \!\left(\frac{k_n}{D}\right)^2} \, M\psi_{ij} \, \frac{1}{r_{ij}} \, \frac{\partial}{\partial r_{ij}} \, F(r_{ij})$$

$$- \frac{2\nu}{\displaystyle\sum_{n=0}^{8} A_n \!\left(\frac{k_n}{D}\right)^2} \, M\chi_{ij} \, \frac{\partial^2}{\partial r_{ij}^2} \, F(r_{ij})$$

(2.3.18)

and similarly for the transverse component

$$corr\!\left(u_i^t \, u_j^t\right) = - \frac{2(1-\nu)}{\displaystyle\sum_{n=0}^{8} A_n \!\left(\frac{k_n}{D}\right)^2} \, M\chi_{ij} \, \frac{\partial^2}{\partial r_{ij}^2} \, F(r_{ij})$$

$$- \frac{2\nu}{\displaystyle\sum_{n=0}^{8} A_n \!\left(\frac{k_n}{D}\right)^2} \, M\chi_{ij} \, \frac{1}{r_{ij}} \, \frac{\partial}{\partial r_{ij}} \, F(r_{ij})$$

(2.3.19)

Using the expressions (2.3.12 and 13) for the derivatives of F gives:

$$corr\left(u_i^{\prime}\ u_j^{\prime}\right) = \frac{1}{\beta}\left\{\nu M\chi_{ij}\Sigma_2^0 + \left((1-\nu)\ M\chi_{ij} - \nu M\chi_{ij}\right)\frac{1}{r_{ij}}\Sigma_1^1\right\} \qquad (2.3.20)$$

$$corr\left(u_i^{\prime}\ u_j^{\prime}\right) = \frac{1}{\beta}\left\{(1-\nu)M\chi_{ij}\Sigma_2^0 + \left(\nu M\chi_{ij} - (1-\nu)M\chi_{ij}\right)\frac{1}{r_{ij}}\Sigma_1^1\right\} \qquad (2.3.21)$$

The series is truncated at radial mode 8 (N=8) where

$$\beta = \frac{1}{2}\sum_{n=1}^{N} A_n \left(\frac{k_n}{D}\right)^2$$

$$\Sigma_2^0 = \sum_{n=1}^{N} A_n \left(\frac{k_n}{D}\right)^2 J_0\left(\frac{k_n}{D} r_{ij}\right)$$

$$\Sigma_1^1 = \sum_{n=1}^{N} A_n \left(\frac{k_n}{D}\right) J_1\left(\frac{k_n}{D} r_{ij}\right)$$

J_1 is the Bessel function of first order and first kind. The series is truncated at radial mode 8($N=8$).

Spherical geometry is employed throughout the analysis. For two-point correlations (between a and b) the distance between the points as well as the directions relative to the two local cartesian systems need to be computed.

The two points (radius vectors) on the sphere have the following coordinates in a cartesian system at the centre of the sphere:

$$\bar{a} = R\ (\cos\lambda_a\ \cos\theta_a,\ \sin\lambda_a\ \cos\theta_a,\ \sin\theta_a)$$

$$\bar{b} = R\ (\cos\lambda_b\ \cos\theta_b,\ \sin\lambda_b\ \cos\theta_b,\ \sin\theta_b)$$

where λ and θ are longitudes and latitudes. The angle between α between $\bar{a}$ and $\bar{b}$ is from the scalar product $\bar{a}.\bar{b}$:

$$\alpha = \arccos\ [\cos\lambda_a\ \cos\lambda_b\ \cos\theta_a\ \cos\theta_b + \sin\lambda_a\ \cos\theta_a\ \sin\lambda_b\ \cos\theta_b + \sin\theta_a\ \sin\theta_b] \qquad (2.3.22)$$

and the great circle distance is

αR (or just α in radians).

The vector $\overline{ab}$ between the points is

$$\overline{ab} = R \ (\cos\lambda_b \ \cos\theta_b - \cos\lambda_a \ \cos\theta_a, \ \sin\theta_b \ \cos\theta_b - \sin\lambda_a \ \cos\theta_a, \ \sin\theta_b - \sin\theta_a)$$

The axis vectors in the local cartesian system (at a or b) can be written (local north and east)

$$\overline{N} = (-\cos\lambda \ \sin\theta, \ - \sin\lambda \ \sin\theta, \ \cos\theta)$$

$$\overline{E} = (-\sin\lambda, \ \cos\lambda, \ 0)$$

The vector $\overline{ab}$ is then projected onto the local tangent plane defined by $\overline{N}$ and $\overline{E}$;

$$\overline{ab'} = (\overline{ab}.\overline{N})\overline{N} + (\overline{ab}.\overline{E})\overline{E}$$

then the angle α between $\overline{ab'}$ and $\overline{E}$ can be found through the scalar product:

$$\cos\alpha = \frac{\overline{ab'}.\overline{E}}{\sqrt{(\overline{ab}.\overline{N})^2 + (\overline{ab}.\overline{E})^2}} = \sin\beta \qquad (2.3.23)$$

where β is the angle between $\overline{ab'}$ and $\overline{N}$, local north.

Observed and analysed wind data are represented as local cartesian wind components, u and v. These components need to be projected onto the longitudinal and transverse components (u^l, u^t, v^l and v^t) and the longitudinal and transverse contribution from (2.3.20 and 21) are added.

$$u^l = u \sin\beta, \ v^l = v \cos\beta$$
$$u^t = -u \cos\beta, \ v^t = v \sin\beta$$

with β from (2.3.23).

$$corr(u_i \ u_j) = corr(u_i^l \ u_j^l) \sin\beta_i \sin\beta_j + corr(u_i^t \ u_j^t) \cos\beta_i \cos\beta_j \qquad (2.3.24)$$

$$corr(u_i \ v_j) = corr(u_i^l \ u_j^l) \sin\beta_i \cos\beta_j - corr(u_i^t \ u_j^t) \cos\beta_i \sin\beta_j \qquad (2.3.25)$$

$$corr(v_i \ v_j) = corr(u_i^l \ u_j^l) \cos\beta_i \cos\beta_j + corr(u_i^t \ u_j^t) \sin\beta_i \sin\beta_j \qquad (2.3.26)$$

$$corr(v_i \ u_j) = corr(u_i^l \ u_j^l) \cos\beta_i \sin\beta_j - corr(u_i^t \ u_j^t) \sin\beta_i \cos\beta_j \qquad (2.3.27)$$

Finally, at very small distances ($< \varepsilon$ or $= 0$) the above expressions are replaced by

$$<u_1 \ u_2> = \sin\lambda_1 \ \sin\lambda_2 + \cos\lambda_1 \ \cos\lambda_2 \qquad (2.3.28)$$

$$<u_1 \ v_2> = \sin\lambda_1 \ \cos\lambda_2 - \cos\lambda_1 \ \sin\lambda_2 \qquad (2.3.29)$$

$$<v_1 \ u_2> = \cos\lambda_1 \ \sin\lambda_2 - \sin\lambda_1 \ \cos\lambda_2 \qquad (2.3.30)$$

$$<v_1 \ v_2> = \cos\lambda_1 \ \cos\lambda_2 + \sin\lambda_1 \ \sin\lambda_2 \qquad (2.3.31)$$

λ_1 and λ_2 are the two longitudes which may now be the same (e.g. the North Pole).

A substantial contribution to the wind forecast errors comes from planetary scale waves (*Hollingsworth and, Lönnberg*, 1986). Over an analysis volume, the structure of such waves is essentially constant. The expressions have been modified to accommodate the large scale errors in the following way:

$$<u_i',u_j'> = <u_i',u_j'>_{SYN} + const$$

$$<u_i',u_j'> = <u_i',u_j'>_{SYN} + const$$

$$<u_i',u_j'> = <u_i',u_j'> = 0$$

The synoptic scale correlations (SYN) are given by expressions (2.3.20 and 21). The constant term has a value of 0.15.

This wind error model is suitable for global analyses of the wind field using wind data only.

For multivariate height and wind analyses we need to specify cross- correlations between height (and hence thickness) and wind. If in doing this we were to ensure that the height and wind covariances obey the geostrophic relationship, then the analysed increments within each analysis box would do so also. Ignoring horizontal derivatives of the Coriolis parameter, f, this could be done relating height and streamfunction:

$$\psi_i = \frac{g}{f} h_i$$

$$M_\psi = M_h$$

$$F_\psi = F_h$$

$$E_{\psi_i} = \frac{g}{f} E_{h_i}$$

This precise equivalence is impossible in the tropics since $f\sim 0$ and is undesirable even at high latitudes, since we do not wish to enforce precise obedience of the geostrophic relationship. Instead we define a height streamfunction error correlation $\mu_{h\psi}$ such that $\mu_{h\psi} \leq 1$ in northern hemisphere high latitudes, $\mu_{h\psi} \geq -1$ in southern hemisphere high latitudes and $\mu_{h\psi} = 0$ at the equator.

This removes the need for precise equivalence of height and streamfunction and M, F and E can be specified independently for each. However, as $| \mu_{h\psi} |$ approaches unity we need to ensure that they approximately obey the above relationships in order that the multivariate correlation model is self- consistent and that the analysis increments are in approximate geostrophic balance.

The cross-variance between geopotential and streamfunction is

$$<\Phi_i \psi_j> = \mu E_\Phi E_\psi M_{\Phi\psi} F(r_{ij})$$

The correlation between the transverse wind component and the height is then

$$<u_i' z_j> = -<z_i \mu_j'> = -\mu \frac{E_\Phi E_{\psi}}{E_\Phi E_\psi} M_{\Phi\psi} \frac{\partial F}{\partial r_{ij}}(r_{ij}) \qquad (2.3.32)$$

and from (2.3.7):

$$<u_i' z_j> = -<z_i \mu_j'> = -\mu \sqrt{1-v} \, M_{\Phi\psi} \frac{\partial F(r_{ij})}{\partial r_{ij}} \qquad (2.3.33)$$

To facilitate the geostrophic coupling $M_{\Phi\psi}$ is chosen to be the same as $M_\psi = M_h$.

Examples of the resulting cross correlations of different variables in the extra tropics are shown in Fig. 2.2.

2.3.5 Practical generation of height thickness and wind covariance

The mass and wind analysis computations are organised in such a way that it is convenient to separate all the covariances into errors and correlations. In this section we describe the method used to generate the values required from the available empirical data and past experience in such a way as to ensure that the requirements of (2.3.2) to (2.3.4) are met. First we outline the steps, then describe in more detail the data currently in use.

a)   Specify a smooth global three-dimensional E_h field.

b)   Specify two-dimensional global values of M_h.

c)   Calculate from E_h and M_h a global three-dimensional $E_{\Delta H}$ field, and extend the M_h matrices to contain $h-\Delta h$ and $\Delta h-\Delta h$ correlations.

d)   Specify a smooth global three-dimensional L_h field.

e)   Specify a smooth global three-dimensional $\mu_{h\psi}$ field.

f)   Calculate $E_{u,v}$ from $E_{u,v} = \frac{g}{\sqrt{2}Lf} E_h$ where $|\mu_{h\psi}|$ is large. Specify $E_{u,v}$ independently where $|\mu_{h\psi}|$

is small, ensuring a smooth global field.

g)   Define $M_\psi = H_h$ where $|\mu_{h\psi}|$ is large. Specify M_ψ independently in the tropics where $|\mu_{h\psi}|$ is small. Calculate everywhere a complete vertical correlation matrix M of ψ, h and Δh

h)   Define $L_\psi = L_h$ everywhere.
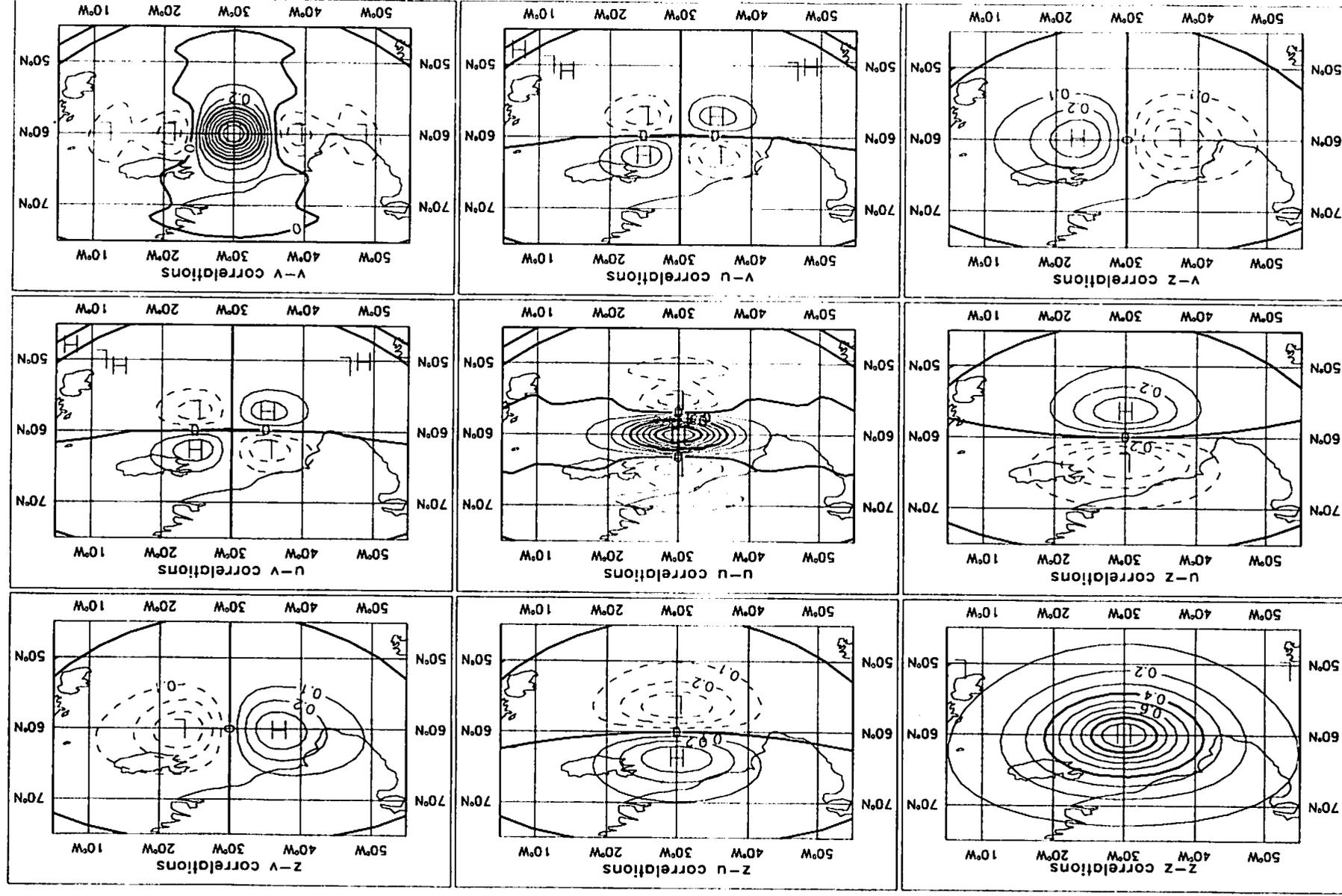
2.3.5(a)   *Details on implementation*

The forecast error covariances in use in the ECMWF analysis scheme have been determined from past performance of the ECMWF assimilation system as verified against radiosondes (*Hollingsworth and Lönnberg*, 1986; *Lönnberg and Hollingsworth*, 1986).

Vertical forecast error covariances

The empirically determined prediction error covariances contain noise that must be filtered in order to ensure positive definiteness. It is therefore desirable to model the empirical data by a positive definite function. An exponential model that takes the local scale height of the error into account has been suggested by *Cats* (1982). This model uses only the error correlations between adjacent levels and the variances at 15 levels to construct a full matrix.

The correlation matrix is constructed as follows:

(i)   Prescribe the first off-diagonal correlations (from empirical results) $c_{i,i-1}$, $i=2$, ..., 15

(ii)   Assign $x_1 = 0$ (arbitrary) and $x_i = x_{i-1} + (-\ell n\ c_{i,i-1})^{1/\sigma}$, $i=2$, ..., 15

(iii)   Calculate all correlations

$$c_{ij} = \exp[-|\ x_i - x_j|^\sigma]\ i=1,\ ...,\ 15 \text{ and } j=1,\ ...,\ 15$$

$\sigma = 1.6$ gives reasonably good approximation to empirical correlations.

The basic set of forecast error covariances, mid-latitude winter and summer height error covariances and tropical wind and height errors, as well as divergent wind correlations, are given in Tables 2.1 to 2.8.

The covariance matrices are split into variances and correlations. In extratropical regions the variances are interpolated in time using a sine function. The interpolation of correlations is linear in time. The same matrices are used throughout the year in the tropics ($10°N$ to $10°S$). The mid-latitude wind matrices are derived from the mid-latitude height matrices by geostrophy and the horizontal correlations of height errors. The interpolated variances and correlations are combined and the resulting covariance matrices are checked for positive definiteness. If the matrices are not positive definite, the offending eigenvalues are altered and the matrices reconstructed.

The next step is a latitudinal interpolation of covariances for a given month. The covariance matrices are again split into errors and correlations. The correlation matrices are interpolated linearly to produce matrices for each latitude band of the error grid ($6°$ latitude). The errors are interpolated smoothly (simulating the climatological variance) to produce errors for each latitude. Consistent correlations and errors are then

produced for other variables (wind and thickness), taking into account the assumed model for horizontal correlation of errors, and geostrophy in mid-latitudes.

The final correlation matrix for all variables is also checked for positive definiteness and modified if necessary, by altering eigenvalues and off- diagonal, cross-correlation, terms.

Horizontal forecast error scales

The scale length L defined in Section 2.3.2 is the ratio of the streamfunction (or velocity potential) variance to the sum of the variances of the two velocity components, i.e. the associated vector wind variance. The 'component' length scale L_c is the length scale which defines the ratio of the streamfunction amplitude to the corresponding rms velocity component. Until May 1985 ECMWF used an auto-correlation function in the form (*Lorenc*, 1981)

$$F(r) = \exp\left[-\frac{1}{2}\left(\frac{r}{L_c}\right)^2\right]$$

Z correlations (*1000) and errors (m/s)

	1000	850	700	500	400	300	250	200	150	100	70	50	30	20	10
1000	1000	442	199	105	80	58	48	38	29	22	19	·17	15	13	11
850	442	1000	576	244	168	109	84	63	45	32	27	24	21	17	14
700	199	576	1000	564	358	205	147	101	67	45	36	32	27	22	17
500	105	244	564	1000	834	468	306	188	112	68	52	45	37	29	22
400	80	168	358	834	1000	730	479	278	154	87	65	55	44	35	25
300	58	109	205	468	730	1000	848	508	254	129	91	75	58	44	31
250	48	84	147	306	479	848	1000	768	382	177	120	96	73	54	36
200	38	63	101	188	278	508	768	1000	666	284	179	138	100	70	45
150	29	45	67	112	154	254	382	666	1000	575	335	243	162	106	63
100	22	32	45	68	87	129	177	284	575	1000	780	564	343	198	102
70	19	27	36	52	65	91	120	179	335	780	1000	896	589	319	147
50	17	24	32	45	55	75	96	138	243	564	896	1000	808	450	192
30	15	21	27	37	44	58	73	100	162	343	589	808	1000	731	295
20	13	17	22	29	35	44	54	70	106	198	319	450	731	1000	541
10	11	14	17	22	25	31	36	45	63	102	147	192	295	541	1000
	8.0	7.9	9.1	12.6	14.8	16.7	17.2	17.2	16.5	15.3	15.5	17.9	26.5	36.6	50.0

Table 2.1 Vertical forecast error correlations (x 1000) and mean forecast error standard deviations of height (m) at 15 standard levels. Values are for extratropical winter.

Z correlations (*1000) and errors (m/s)

	1000	850	700	500	400	300	250	200	150	100	70	50	30	20	10
1000	1000	443	187	89	64	44	35	26	19	12	9	7	5	4	3
850	443	1000	533	192	124	76	56	40	26	16	11	8	6	5	4
700	187	533	1000	459	258	135	92	60	36	20	13	10	7	6	4
500	89	192	459	1000	743	333	197	110	58	28	18	12	8	7	5
400	64	124	258	743	1000	604	335	167	78	35	21	14	9	7	5
300	44	76	135	333	604	1000	748	338	130	49	27	18	11	8	6
250	35	56	92	197	335	748	1000	610	202	64	33	21	13	9	7
200	26	40	60	110	167	338	610	1000	426	101	45	27	15	11	8
150	19	26	36	58	78	130	202	426	1000	238	80	41	21	15	9
100	12	16	20	28	35	49	64	101	238	1000	287	99	39	24	14
70	9	11	13	18	21	27	33	45	80	287	1000	336	80	42	21
50	7	8	10	12	14	18	21	27	41	99	336	1000	210	82	33
30	5	6	7	8	9	11	13	15	21	39	80	210	1000	344	78
20	4	5	6	7	7	8	9	11	15	24	42	82	344	1000	195
10	3	4	4	5	5	6	7	8	9	14	21	33	78	195	1000
	6.8	6.1	6.4	8.0	9.0	9.9	10.0	9.9	9.4	8.9	9.2	10.7	14.9	19.2	24.9

Table 2.2 As Table 2.1 but for extratropical summer.

Z correlations (*1000) and errors (m/s)

	1000	850	700	500	400	300	250	200	150	100	70	50	30	20	10
1000	1000	632	285	117	81	57	48	40	33	25	20	17	13	11	8
850	632	1000	611	207	131	86	70	56	44	33	26	21	16	13	9
700	285	611	1000	438	245	144	111	86	64	45	34	26	19	16	11
500	117	207	438	1000	735	381	267	185	124	77	54	40	27	21	14
400	81	131	245	735	1000	698	482	314	194	111	73	52	34	26	17
300	57	86	144	381	698	1000	880	609	353	177	107	72	44	33	20
250	48	70	111	267	482	880	1000	846	515	243	138	88	52	38	22
200	40	56	86	185	314	609	846	1000	777	363	191	115	64	45	26
150	33	44	64	124	194	353	515	777	1000	626	307	170	86	57	31
100	25	33	45	77	111	177	243	363	626	1000	665	334	141	86	41
70	20	26	34	54	73	107	138	191	307	665	1000	681	250	135	56
50	17	21	26	40	52	72	88	115	170	334	681	1000	488	233	80
30	13	16	19	27	34	44	52	64	86	141	250	488	1000	629	156
20	11	13	16	21	26	33	38	45	57	86	135	233	629	1000	299
10	8	9	11	14	17	20	22	26	31	41	56	80	156	299	1000
	5.7	5.9	6.3	7.6	8.7	10.2	11.1	12.3	13.6	15.2	16.6	18.2	21.8	26.2	35.1

Table 2.3   As Table 2.1 but for the tropics.

U correlations (*1000) and errors (m/s)

	1000	850	700	500	400	300	250	200	150	100	70	50	30	20	10
1000	1000	373	137	57	39	25	20	15	11	7	6	5	4	4	3
850	373	1000	418	116	69	41	30	22	15	10	7	6	5	4	4
700	137	418	1000	295	142	70	48	32	20	12	9	7	6	5	4
500	57	116	295	1000	561	188	107	60	33	18	12	9	7	6	5
400	39	69	142	561	1000	423	204	98	48	23	15	11	8	7	6
300	25	41	70	188	423	1000	619	229	85	34	20	14	10	9	7
250	20	30	48	107	204	619	1000	488	142	47	26	17	12	10	8
200	15	22	32	60	98	229	488	1000	336	77	37	24	16	13	10
150	11	15	20	33	48	85	142	336	1000	197	69	38	23	19	14
100	7	10	12	18	23	34	47	77	197	1000	273	102	49	36	24
70	6	7	9	12	15	20	26	37	69	273	1000	373	116	75	44
50	5	6	7	9	11	14	17	24	38	102	373	1000	329	173	82
30	4	5	6	7	8	10	12	16	23	49	116	329	1000	653	221
20	4	4	5	6	7	9	10	13	19	36	75	173	653	1000	441
10	3	4	4	5	6	7	8	10	14	24	44	82	221	441	1000
	1.7	1.8	2.2	3.2	3.8	4.5	4.8	5.0	4.9	4.3	3.6	3.2	3.3	4.1	4.8

Table 2.4   Non-divergent part of wind forecast error correlations (x 1000) and total wind component forecast error standard deviations (m/s) in the tropics.

barotropic Z correlations (*1000)

	1000	850	700	500	400	300	250	200	150	100	70	50	30	20	10
1000	1000	878	633	341	232	139	96	57	25	6	2	1	0	0	0
850	878	1000	905	633	487	336	255	170	89	28	9	3	1	1	0
700	633	905	1000	878	753	589	483	357	215	83	32	13	5	3	1
500	341	633	878	1000	971	874	785	652	461	228	107	52	23	15	4
400	232	487	753	971	1000	962	902	792	606	336	173	91	43	29	9
300	139	336	589	874	962	1000	985	921	769	487	280	161	82	59	21
250	96	255	483	785	902	985	1000	974	861	593	365	222	120	89	34
200	57	170	357	652	792	921	974	1000	950	730	492	321	188	143	59
150	25	89	215	461	606	769	861	950	1000	894	684	494	320	255	120
100	6	28	83	228	336	487	593	730	894	1000	924	775	585	499	286
70	2	9	32	107	173	280	365	492	684	924	1000	951	816	737	495
50	1	3	13	52	91	161	222	321	494	775	951	1000	950	897	685
30	0	1	5	23	43	82	120	188	320	585	816	950	1000	990	861
20	0	1	3	15	29	59	89	143	255	499	737	897	990	1000	922
10	0	0	1	4	9	21	34	59	120	286	495	685	861	922	1000

Table 2.5   Vertical forecast error correlations (x 1000) of the large-scale height error. These values are used globally.

/

divergent U correlations (*1000) and errors (m/s)

	1000	850	700	500	400	300	250	200	150	100	70	50	30	20	10
1000	1000	189	-135	-232	-247	-250	-246	-235	-218	-196	-183	-174	-163	-150	-132
850	189	1000	380	-79	-171	-229	-246	-251	-243	-225	-211	-202	-190	-175	-154
700	-135	380	1000	363	73	-128	-194	-235	-251	-243	-232	-224	-212	-196	-173
500	-232	-79	363	1000	755	227	3	-147	-227	-251	-248	-243	-233	-219	-195
400	-247	-171	73	755	1000	604	243	-34	-186	-244	-251	-249	-243	-230	-207
300	-250	-229	-128	227	604	1000	775	284	-66	-212	-242	-249	-250	-243	-222
250	-246	-246	-194	3	243	775	1000	658	106	-161	-220	-239	-250	-249	-232
200	-235	-251	-235	-147	-34	284	658	1000	510	-27	-158	-203	-236	-250	-244
150	-218	-243	-251	-227	-186	-66	106	510	1000	379	42	-79	-177	-231	-251
100	-196	-225	-243	-251	-244	-212	-161	-27	379	1000	675	362	53	-136	-234
70	-183	-211	-232	-248	-251	-242	-220	-158	42	675	1000	846	399	21	-194
50	-174	-202	-224	-243	-249	-249	-239	-203	-79	362	846	1000	717	201	-143
30	-163	-190	-212	-233	-243	-250	-250	-236	-177	53	399	717	1000	605	-12
20	-150	-175	-196	-219	-230	-243	-249	-250	-231	-136	21	201	605	1000	330
10	-132	-154	-173	-195	-207	-222	-232	-244	-251	-234	-194	-143	-12	330	1000
	1.3	1.3	1.5	2.1	2.5	2.8	2.9	2.9	2.8	2.6	2.6	3.0	4.5	6.2	8.4

Table 2.6   Divergent part of the wind forecast error correlation (x 1000) and total wind component forecast error standard deviation (m/s) for extratropical winter.

divergent U correlations (*1000) and errors (m/s)

	1000	850	700	500	400	300	250	200	150	100	70	50	30	20	10
1000	1000	165	-180	-270	-274	-261	-246	-223	-189	-147	-118	-98	-77	-66	-53
850	165	1000	297	-173	-245	-274	-271	-255	-221	-172	-138	-114	-89	-75	-60
700	-180	297	1000	191	-89	-235	-268	-273	-249	-197	-158	-129	-100	-84	-66
500	-270	-173	191	1000	610	11	-167	-257	-272	-229	-184	-151	-115	-96	-75
400	-274	-245	-89	610	1000	402	14	-203	-273	-246	-201	-164	-125	-104	-81
300	-261	-274	-235	11	402	1000	617	18	-241	-266	-224	-185	-140	-116	-89
250	-246	-271	-268	-167	14	617	1000	410	-162	-274	-241	-201	-152	-126	-96
200	-223	-255	-273	-257	-203	18	410	1000	141	-263	-262	-224	-171	-141	-107
150	-189	-221	-249	-272	-273	-241	-162	141	1000	-116	-273	-257	-202	-166	-125
100	-147	-172	-197	-229	-246	-266	-274	-263	-116	1000	-52	-264	-253	-214	-161
70	-118	-138	-158	-184	-201	-224	-241	-262	-273	-52	1000	16	-273	-258	-201
50	-98	-114	-129	-151	-164	-185	-201	-224	-257	-264	16	1000	-151	-272	-242
30	-77	-89	-100	-115	-125	-140	-152	-171	-202	-253	-273	-151	1000	29	-273
20	-66	-75	-84	-96	-104	-116	-126	-141	-166	-214	-258	-272	29	1000	-170
10	-53	-60	-66	-75	-81	-89	-96	-107	-125	-161	-201	-242	-273	-170	1000
	0.9	0.8	0.9	1.1	1.2	1.3	1.3	1.3	1.3	1.2	1.2	1.4	2.0	2.6	3.4

Table 2.7   As Table 2.6 for extratropical summer.

divergent U correlations (*1000) and errors (m/s)

	1000	850	700	500	400	300	250	200	150	100	70	50	30	20	10
1000	1000	115	-181	-233	-222	-198	-180	-157	-131	-101	-83	-71	-61	-57	-50
850	115	1000	175	-201	-232	-225	-209	-186	-155	-119	-97	-83	-70	-65	-57
700	-181	175	1000	11	-176	-232	-230	-212	-181	-139	-112	-95	-80	-74	-65
500	-233	-201	11	1000	374	-125	-209	-233	-215	-170	-138	-116	-97	-88	-77
400	-222	-232	-176	374	1000	183	-106	-216	-230	-190	-155	-130	-108	-99	-86
300	-198	-225	-232	-125	183	1000	456	-74	-225	-216	-180	-152	-126	-114	-99
250	-180	-209	-230	-209	-106	456	1000	271	-177	-230	-198	-169	-140	-127	-110
200	-157	-186	-212	-233	-216	-74	271	1000	64	-229	-220	-192	-160	-145	-125
150	-131	-155	-181	-215	-230	-225	-177	64	1000	-114	-232	-222	-192	-175	-151
100	-101	-119	-139	-170	-190	-216	-230	-229	-114	1000	-19	-213	-231	-219	-195
70	-83	-97	-112	-138	-155	-180	-198	-220	-232	-19	1000	114	-201	-230	-228
50	-71	-83	-95	-116	-130	-152	-169	-192	-222	-213	114	1000	55	-142	-227
30	-61	-70	-80	-97	-108	-126	-140	-160	-192	-231	-201	55	1000	503	-85
20	-57	-65	-74	-88	-99	-114	-127	-145	-175	-219	-230	-142	503	1000	207
10	-50	-57	-65	-77	-86	-99	-110	-125	-151	-195	-228	-227	-85	207	1000
	1.7	1.8	2.2	3.2	3.8	4.5	4.8	5.0	4.9	4.3	3.6	3.2	3.3	4.1	4.8

Table 2.8   As Table 2.6 for the tropics.

The value of the length scale is constant in pressure but depends on latitude:

$L_z - \sqrt{\overline{z'^2}}$		L
90° - 30°N	400 km	354 km
30 - 24°N	446 km	424 km
24 - 18°N	486 km	495 km
18 - 12°N	526 km	566 km
12 - 6°N	560 km	636 km
6°N - 6°S	600 km	707 km
6 - 12°S	560 km	636 km
12° - 18°S	520 km	566 km
18 - 24°S	500 km	495 km
24 - 90°S	500 km	424 km

Height-streamfunction correlations

The following height streamfunction correlation model is used:

$$\mu_{z\psi} - \mu_0 = \begin{cases} \mu_0 & \phi > \phi_c \\[4pt] -\mu_0 \sin\left(\frac{\pi}{2}\,\frac{\phi}{\phi_c}\right) & -\phi_c < \phi < \phi_c \\[4pt] -\mu_0 & -\phi_c > \phi \end{cases} \qquad (2.3.9)$$

Where ϕ is the latitude. The values currently used are $\mu_0 = .90$ and $\phi_c = 30°$ for modes 1-5. Mode 6 has a correlation of 0.45 and modes 7 and 8 no geostrophic coupling at all.

Wind error covariances

E_n is calculated geostrophically for $|\phi| > \phi_{crit}$, and a smooth field is specified in the tropics, based on the past performance of the ECMWF assimilation system in the tropics.

$M_\psi - M_{zn}$ is assumed in extratropical areas. The tropical vertical correlations have been derived by verifying the six hour forecasts against radiosondes.

$L_\psi - L_z$ is assumed globally.

The vertical forecast error correlations are widened over the North Pacific (25°-60° N: 140° E-120° W), the North Atlantic (25°-70° N: 80° W-10° W) and Southern Hemisphere extratropics (south of 25° S). The vertical correlation function (2.3.14) is modified by multiplying the constant a by 2 (or 1.5 in a transition zone).

2.3.5(b)   *Data sources*

Forecast error covariances

Mid-latitude and tropical geopotential height and wind forecast error covariances have been calculated by verifying the six hour forecasts against radiosonde observations (*Hollingsworth and Lönnberg*, 1986; *Lönnberg and Hollingsworth*, 1986). The error covariances have been estimated for both winter and summer seasons. A further revision and increase of resolution was done by *Lönnberg*, 1988).

Climatological error covariances

- Winter (January), mid-latitude (61°N) geopotential climatology error covariances for WMO station Jokioinen, Finland

- Tropical (10°N and 10°S) geopotential height climatology error covariances constructed from variances and correlations:

  a) variances: mean yearly climatological variances from 10°N to 10°S from *Oort and Rasmussen* (1971).

  b) correlations: yearly climatological correlations of geopotential height at Port Hedland, Australia, from *Maher and Lee* (1977).

- Tropical (10°N to 10°S) wind climatology error covariances constructed from variances and correlations:

  a) variances: mean yearly climatological variances of vector wind from 10°N to 10°S from *Oort and Rasmussen* (1971).

  b) correlations: yearly climatological correlations of zonal wind or altitude surfaces at Port Hedland, Australia, from *Maher and Lee* (1977).

2.3.6   Modification of first-guess errors for each analysis

Global three-dimensional fields of E_h, $E_{\Delta h}$, $E_{u,v}$, $\mu_{h,\psi}$ and L, and a matrix $M_{h,\,\Delta h,\,\psi}$ are constructed for each month through the procedures of Section 2.3.5. The monthly mean errors are derived from data sources which are representative for geographical regions with a dense observation network. Consequently, a modification of the mean forecast error is necessary for each analysis time due to spatial and temporal variations in the data density. The analysis errors are calculated on a 6° x 6° latitude-longitude grid at 7 levels (1000, 500, 300, 200, 100, 50 and 10 hPa).

However, the forecast errors and correlations are not independent but coupled by the equations linking the height and thickness covariances and the height and wind errors. A multiplication of the errors by a horizontally varying error factor is possible without having to recalculate $M_{h,\,\Delta h,\,\psi}$. Such a factor is calculated from the analysis error of the previous analysis by the following procedure:

(i) Calculate the ratios of the analysis errors for u, v and h over the estimated prediction errors $E_{u,v}$ and E_h, and average over 7 levels ($j = 1, ..., N$) and all variables ($i = u, v, h$), to give a two-dimensional analysis error factor field:

$$e^a = \frac{1}{3N} \sum_{i=1}^{3} \sum_{j=1}^{N} \frac{E_{ij}^a}{E_{ij}^{fc}}$$

(2.3.10)

E^a is the analysis error as estimated by (2.2.6) and E^{fc} are the mean forecast errors of Section 2.3.5.

(ii) Similarly, calculate the error factor field of the mean ratio of the climatological standard deviation for u, v and h over the $E_{u,v}$ and E_h:

$$e^c = \frac{1}{3N} \sum_{i=1}^{3} \sum_{j=1}^{N} \frac{E_{ij}^{clim}}{E_{ij}^{fc}}$$

(2.3.11)

(iii) Let the mean analysis error factor e^a grow linearly to the error level of a random state in time Δt_{rand}:

$$e^{mod} = e^a + \frac{\Delta t_{fc}}{\Delta t_{rand}} \left(\sqrt{2} \, e^c - e^a \right)$$

(2.3.12)

Δt_{rand} must be chosen in such a way that $e^{mod} \sim 1$ for an observation density similar to that used in the calculation of the mean forecast errors. This gives a value of $\Delta t_{rand} = 6$ days in mid-latitudes and 2 days in tropics for $\Delta t_{fc} = 6$ hours. A 2-dimensional filter is applied to the e^{mod}- field.

(iv) Multiply the monthly fields E_h, $E_{\Delta h}$, $E_{u,v}$ by the factor to give the errors actually to be used for the next analysis for each analysis box:

$$\left(E_{ij}^{fc} \right)^{mod} = e^{mod} \, E_{ij}^{fc}$$

(2.3.13)

2.3.7 Functional representation of horizontal and vertical correlations

2.3.7(a) *Horizontal correlation model*

The evaluation of Bessel functions is extremely expensive and it has been necessary to approximate each of the sums of Bessel functions in (2.3.8) by Pade polynomials (ratio of two polynomials).

2.3.7(b) *Vertical covariance model*

The forecast errors of heights and winds are expressed as polynomials in $\ell n(p)$. A sixth degree polynomial is fitted to the forecast errors at 15 standard pressure levels.

The vertical correlation matrix which has been constructed according to the principles outlined in Section 2.3.5(a) is used in a least squares fit to a continuous functional expression (*Undén*, 1984).
The correlation model is

$$c_{i,j} = \frac{1}{e-1} \exp\left[\frac{a}{a+(x_i-x_j)^2}\right] - \frac{1}{e-1} \qquad (2.3.14)$$

where $c_{i,j}$ is the correlation between levels i and j, e-exp(1), a is a tuning constant and x_i, x_j are transformed vertical coordinates.

For the divergent wind 2.3.14 is modified to

$$c_{i,j} = \left\{\frac{1}{e-1} \exp\left[\frac{a}{a+(x_i-x_j)^2}\right] - \frac{1}{e-1}\right\} \cdot \frac{1-0.75(x_i-x_j)^2}{1+0.04(x_i-x_j)^2} \qquad (2.3.15)$$

The values of x_i define the coordinate transformation from the pressure levels and can be found by setting $j=i-1$ in (2.3.14).

$$x_1 = 0$$

$$x_i - x_{i-1} = \sqrt{\frac{a}{\ln\left(\frac{c_{i,j}+b}{b}\right)} - a} \text{ where } b = \frac{1}{e-1} \qquad (2.3.16)$$

The steps for constructing the continuous representation of forecast errors and correlations from a discrete covariance matrix are as follows:

(i)   Fit the height forecast errors at pressure levels to a sixth degree polynomial.

(ii)   Take the calculated height error correlations ($c_{i,j}$) between adjacent pressure levels and compute the transformed vertical coordinates, x_i, for all levels using (2.3.16) with a first guess value of parameter a. The x_i's are then fitted to a sixth order polynomial in $\ell n(p)$ to give a continuous representation.

(iii)   With correlation model (2.3.14) and the functional expression of x from (ii), find a new value of parameter a which fits the two off-diagonal correlations, i.e. $c_{i,i+1}$ and $c_{i,i+2}$, as well as $c_{i,i-1}$ and $c_{i,i-2}$ where applicable.

2.4   OBSERVATIONS AND OBSERVATION ERROR STATISTICS

2.4.1   The analysis observation file

All appropriate types of available observations are used in the analysis. Data are presented in the form of an analysis observation file which includes all reports for a 6 hr period spanning the nominal analysis time. To be precise, the 12GMT analysis uses data in the time range 0901-1500 GMT inclusive; the other three analysis times have corresponding ranges. In operations the analysis observation file is produced from the Centre's Reports Data Base which in turn is built up from data received via the Centre's links into the GTS. For FGGE analyses the analysis observation file is produced from data received from the appropriate Data Centre.

2.4.2   Processing of observed data

The analysis equations assume that all data are processed to give observed minus first-guess values for wind components, geopotential height and thickness. The procedures used to derive these values from the observation report and the first-guess field are described in this section.

2.4.2(a)   *Interpolation of first-guess*

For each observation the first-guess field is interpolated to the observation position. The vertical interpolation is done at the four nearest grid points to the pressure of the observation. For details of the vertical interpolation see Section 5.1. The horizontal interpolation is bilinear at constant pressure. 3, 6 and 9 hour forecasts are used as first guesses. The observation departures are computed for each and then interpolated quadratically in time.

2.4.2(b)   *Multi-level observations*

These are processed in 2 steps:

(i)   Process all levels in report.

(ii)   Define a set of levels around which one entry is selected. The levels are: 1000-850-700-500-400-300-250-200-150-100-70-50-30-20-10 hPa. The selection gives preference to the entry closest to one of the above levels. The search for an entry extends halfway between two levels. Satellite thicknesses however are presented to the analysis for the following layers: 1000-700-500-300-100-50-30-10 hPa.

2.4.2(c)   *Upper-air single level observations*

Only the wind from these is used at the reported pressure.

2.4.2(d)   *Surface observations*

As well as the pressure level first-guess values used for other observations, the first-guess file contains 10 metre wind values obtained directly from the forecast model. These are used to give the first-guess for surface wind. For observations reporting sea level pressure, a first-guess height value is calculated at observed pressure. The height departure, $z_{obs}(=0)-z_{fg}$, is used at the reported sea level pressure. Stations reporting an alternative to sea level pressure are treated consistently with this. The wind increment obtained is assigned to the reported pressure. Winds from ships and from tropical ($30°N-30°S$) low level (both station height and model orography are less than 150 m) land stations are used; winds from other land stations are not used. The station height information is based on the WMO Vol.A catalogue of observing stations, with some modification of those station heights which separate studies have shown to be wrong. Apart from this use of the model's surface winds as first guess, no allowance is made for the effect of surface friction on observed winds.

The use of single level height observations (SYNOP and DRIBU) at their reported pressures leads to systematic spurious temperature increments. To overcome this problem, each such datum is complemented by an artificial thickness datum with zero departure from the first-guess in the main analysis. The thickness is over 10 hPa and uses the same normalised observation error as the original height datum. This means that we impose a weak constraint on the analysis to use the first-guess temperature when only single level height data are available.

If more than one observation is available from a station, then the one closest in time is selected.

2.4.2(e)   *Types of observations*

All appropriate types of observations are used in the analysis. They are: reports from surface land and sea platforms (SYNOPs and SHIPs); radio sonde and pilot reports (TEMPs and PILOTs); satellite wind reports (SATOBs); aircraft reports (AIREPs); satellite thickness reports (SATEMs); drifting buoy reports (DRIBUs); and when available, winds from constant level balloons (COLBAs), and drop-sondes (TEMPDROPs). The SYNOP/SHIP category includes observations from automatic stations and stations reporting in abbreviated/reduced form.

The AIREP category includes automated wind measurements (ASDARs, and when available, AIDS). The positions of all land stations are taken from the WMO Vol.A catalogue.

No satellite wind data over extratropical land areas (polewards of latitude 20°) are used. No tropospheric satellite thickness data over land areas are used; however SATEM thickness data above 100 mb over land are used. SATEMs transmitted on GTS have a horizontal resolution of 500 km. In addition satellite observations with approximately 120 km horizontal resolution are transmitted from Washington. These observations are usually called TOVS.

In addition to these real reports, the operational analysis can make use of bogus data (PAOBs) supplied by the Melbourne WMC. The use of PAOBs is restricted to ocean regions south of 19°S and only the surface pressure value of the PAOB is used (the 1000-500 mb thickness information in the PAOB is not used). At present they are not decoded.

A second facility exists to either exclude from the analysis observation file, or to include it with a flag 3, any data source considered to be 'permanently' wrong.

2.4.3 Observation error statistics

2.4.3(a) *Error variances*

Error variances of geopotential and (component) wind are required for each observation type at any level. For the SATEM data an error variance of geopotential thickness for the layer between analysis levels is required. The values used, expressed as rms errors, are shown in Tables 2.9 (a) and (b). They have been derived by statistical evaluation of the performance of the observing systems, as components of the assimilation system, over long periods of operational use. The observation error is interpolated linearly in $\ln p$ to the reported pressure. Above 10 hPa and below 1000 hPa, the observation error is assumed constant.

The normalised observation error e^o in (2.2.2) is not allowed to fall below 0.5 for numerical conditioning reasons.

2.4.3(b) *Error correlations*

As described in Section 2.2.1, account must be taken of observational error correlations. Such correlations are deemed to arise from three differing observational characteristics. The first is the vertical correlation of error that typically exists in a TEMP (in geopotential). The second is the vertical correlation of error that typically exists within a SATEM sounding.

The third is the horizontal correlation of error that typically exists in SATEM soundings that neighbour each other and are from the same orbit. For data from different satellites or retrieval types the correlations are set to zero. They are also reduced depending on time difference between observations (= 0 for 5 hours).

level (hPa)	TEMP z			TEMP u/v	AIREP	SATOB
	cat 1 (m)	cat 2 (m)	cat 3 (m)	PILOT u/v (m/s)	(m/s)	(m/s)
1000	4.3	6.5	8.6	2.0	3.0	3.0
850	4.4	6.6	8.8	2.4	3.0	3.0
700	5.2	7.8	10.4	2.5	3.0	3.0
500	8.4	12.6	16.8	3.4	3.0	3.0
400	9.8	14.7	19.6	3.6	3.5	6.0
300	10.7	16.1	21.4	3.8	4.0	6.0
250	11.8	17.7	23.6	3.2	4.0	6.0
200	13.2	19.8	26.4	3.2	4.0	6.0
150	15.2	22.8	30.4	2.4	4.0	6.0
100	18.1	27.2	36.2	2.2	4.0	6.0
70	19.5	29.3	39.0	2.0	4.0	6.0
50	22.5	33.8	45.0	2.0	4.0	6.0
30	25.0	37.5	50.0	2.0	4.0	6.0
20	32.0	48.0	64.0	2.5	4.0	6.0
10	40.0	60.0	80.0	3.0	4.0	6.0

Table 2.9 (a) Standard deviations of observation errors for SYNOP, AIREP, SATOB, DRIBU, TEMP, PILOT and PAOB.

SHIP p/z   14.0 m   SYNOP/SHIP wind   3.6 m/s

PAOB p/z   32.0 m   DRIBU wind   5.4 m/s

LAND SYNOP p/z   7.0 m

DRIBU p/z   14.0 m

Cat 1 =   North America (80°-30° N, 50°-170° W)

Cat 2 =   all, except Cat 1 and Cat 3

Cat 3 =   South America (10° N-60° S, 30°-90° W)

Africa, Arabia (30° N-40° S, 20° W-60° E)

layer (hPa)	Clear soundings (m)	Clear soundings (K)	Cloudy soundings (m)	Cloudy soundings (K)
1000/700	27.	2.56	33.	3.13
700/500	17.	1.72	20.	2.02
500/300	25.	1.65	31.	2.05
300/100	53.	1.64	56.	1.74
100/50	33.	1.62	33.	1.62
50/30	36.	2.38	36.	2.38
30/10	74.	2.29	74.	2.29

Table 2.9 (b)   Standard deviations of satellite observation thickness errors and the approximate corresponding temperature errors.

The ascribed vertical error correlation between two pressure levels p_1 and p_2 of geopotential for sondes is given in Table 2.9 (c). These values are then multiplied by a factor of 0.8 when used in the analysis. The actual continuous function used is $a.e^{-b(x_1-x_2)^2}$ where a is 0.8, b a tuning constant close to 1 and x_1 and x_2 are transformation values (based on sixth degree polynomial in lnp) of the two pressures involved.

The error correlation between neighbouring SATEM observations is ascribed to be $a exp$ $(-0.5 \, (\frac{r}{b})^2)$ multiplied by the vertical error correlation, where r is the horizontal separation. Currently $a = .5$ and $b = 300$ km. The vertical error correlation matrix which has been derived by *Kelly* (1985) is showr in Table 2.9 (d). This correlation is only effective when the pair of SATEMs are from the same platform and are of the same retrieval type.

2.4.3(c)   *Adjustments to off-time data*

An adjustment is made to the ascribed observation rms error when the observation in question is asynoptic. The adjusted rms error is

$$E^{o'} = \sqrt{E^{o^2} + E^2_{persis}}$$

where

E^{o^2} =   error variance of the observation

and

E^2_{persis} =   error variance of a persistence forecast for the time difference between observation time and analysis time.

The persistence error is formulated to reflect the dependence on season, distinguishing three regimes - winter hemisphere, tropics and summer hemisphere; and to reflect a dependence on precise latitude within these three regions.

The first part of this dependence is expressed by factors a, b defined as:

$$a = \sin\left(2\pi \, \frac{d}{365.25} + \frac{\pi}{2}\right)$$

$$b = 1.5 + a\{0.5 \, MIN[MAX(\theta, -20), 20] / 20\}$$

where d = day of year

  θ = latitude

radiosonde height error correlations (*1000)

	1000	850	700	500	400	300	250	200	150	100	70	50	30	20	10
1000	1000	716	276	29	5	1	0	0	0	0	0	0	0	0	0
850	716	1000	733	183	55	9	3	1	0	0	0	0	0	0	0
700	276	733	1000	573	268	77	31	10	2	0	0	0	0	0	0
500	29	183	573	1000	851	480	288	138	49	11	3	1	0	0	0
400	5	55	268	851	1000	814	601	364	167	51	19	7	1	0	0
300	1	9	77	480	814	1000	935	738	458	200	93	44	11	2	0
250	0	3	31	288	601	935	1000	919	678	361	194	104	31	7	0
200	0	1	10	138	364	738	919	1000	895	597	375	229	84	24	2
150	0	0	2	49	167	458	678	895	1000	861	649	460	214	78	9
100	0	0	0	11	51	200	361	597	861	1000	929	782	480	230	42
70	0	0	0	3	19	93	194	375	649	929	1000	951	710	412	103
50	0	0	0	1	7	44	104	229	460	782	951	1000	878	598	192
30	0	0	0	0	1	11	31	84	214	480	710	878	1000	881	426
20	0	0	0	0	0	2	7	24	78	230	412	598	881	1000	725
10	0	0	0	0	0	0	0	2	9	42	103	192	426	725	1000

Table 2.9 (c)   Vertical correlations (x 1000) of radiosonde height errors.

SATEM 7-layer vertical correlations for clear soundings							
Layer (hPa)	1000-700	700-500	500-300	300-100	100-50	50-30	30-10
1000-700	1.00						
700-500	0.22	1.00					
500-300	-0.18	0.27	1.00				
300-100	0.00	0.00	-0.16	1.00			
100-50	0.00	0.00	0.16	0.00	1.00		
50-30	0.00	0.00	0.00	0.15	0.00	1.00	
30-10	0.00	0.00	0.00	0.00	0.00	0.27	1.0

Cloudy and Microwave							
Layer (hPa)	1000-700	700-500	500-300	300-100	100-50	50-30	30-10
1000-700	1.00						
700-500	0.22	1.00					
500-300	-0.34	0.22	1.00				
300-100	0.00	-0.25	-0.29	1.00			
100-50	0.00	0.00	0.00	0.00	1.00		
50-30	0.00	0.00	0.00	0.20	0.00	1.00	
30-10	0.00	0.00	0.00	0.00	0.00	0.27	1.0

Table 2.9 (d) Vertical correlations for SATEM observation errors.

The persistence error for a time difference Δt is then expressed as a function of b with a dependence on latitude and a maximum persistence error:

$$E_{persis} = \frac{E_{persis,\ max}}{6} (1 + 2\sin|2\theta|)b\Delta t$$

where Δt is expressed as a fraction of a day and $E_{persis,\ max}$ has the values shown in Table 2.10. The denominator is a scaling factor for $(1 + 2\sin|2\theta|)b$ which has a maximum value of 6.

	1000-700	699-250	249-0 hPa
u, v component (msec^{-1})	6.4	12.7	19.1
Z (m)	48	60	72
T (K)	6	7	8

Table 2.10 Maximum 24 hour persistence error

The error growth rate applied to the pressure datum of an asynoptic surface report is reduced by a factor if the pressure datum has been adjusted using the pressure tendency. The reduction factor is 4 if the pressure tendency correction is for a land station or for a ship whose tendency has also been corrected for ship movement. The reduction factor is 2 if no account of ship movement has been possible.

2.5   QUALITY CONTROL OF DATA

2.5.1   Introduction

Objective methods for the detection of erroneous data are an essential part of an automatic analysis scheme. The checks which can be performed fall into seven different types:

(i)   Checks of code formats etc.

(ii)   Internal consistency checks on the data within one observation.

(iii)   Temporal consistency checks on observations from the same source.

(iv)   Checks that the data are reasonably close to a climatological value.

(v)   Checks that the data are reasonably close to a forecast value.

(vi)   Spatial consistency checks between nearby observations (SYNOPs and SATEMs only).

(vii)   Checks that the data are reasonably close to an analysed value, including dynamic SHIP blacklisting.

At ECMWF checks (i), (ii), and (iv) are performed before the observations are inserted in the data-base ((iii) is not yet implemented) and are outside the scope of this documentation. See "Pre-processing-General: Data checking and validation" by B. Norris, ECMWF Met.Bull. M1.4/3 for details.

Checks (v), (vi) and (vii) are performed during the analysis cycle as a supplement to the other checks. Their purpose is to identify data which would degrade the analysis. Exhaustive tests on all data are not done.

2.5.2 Data flags

Since checks are performed at many different stages of the analysis cycle, it is necessary to carry with each datum flags recording the results of the checks so far. A system of 4 classes is used with the following meaning:

0	correct (or unchecked)
1	probably correct
2	probably incorrect
3	incorrect.

Such a flag is provided for each datum by the data base as a result of checks (i) - (iv) and possibly a manual check. Allowance is also made for manual setting of an override 'certainly correct' flag, which takes precedence over all automatic checks. Although this manual setting facility exists, its use is extremely rare.

The data base flag is taken as the first estimate of an analysis flag, which is then modified as necessary following the checks described below.

2.5.3 Checks performed in mass and wind analysis

2.5.3(a) *Interpretation of data flags*

Rules are needed for the way the observation flags are used to determine the fate of a datum:

(i) Data which have flag 3 are not used.

(ii) Data which have flag 2 and which are not capable of being re-checked by the analysis are not used, e.g. observation position and time (and hence in this case the whole observation is discarded).

(iii) Non-standard level data with a flag 2 from a multi-level observation are not used.
Also SATEM and SATOB data with flag 2 are not used.

(iv) The derived analysis input flag is the maximum flag of the observation data used.

(v) If all of the observation data used have the override (certainly correct) flag set, it is set for the analysis input datum.

2.5.3(b) *Comparison with first-guess*

The analysis input data are transformed into deviations from the first-guess A^p normalized by the estimated first-guess error E:

$$\delta^o = (A^o - A^p)/E^p$$

The estimated observational error E^o is similarly normalised:

$$\epsilon^o - E^o/E^p$$

Each datum is then flagged if its squared deviation is greater than a predetermined multiple $ERRLIM$ of its estimated variance:

$$\text{if } \left(\delta^{o2} > \left(1 + \epsilon^{o2}\right) \times ERRLIM_j\right) \qquad \text{flag} = j \qquad (2.5.1)$$

Wind components are checked and flagged together:

$$\text{if } \left(\frac{\delta_u^{o2} + \delta_v^{o2}}{2}\right) > \left(1 + \frac{\epsilon_u^{o2} + \epsilon_v^{o2}}{2}\right) \times ERRLIM_j \quad \text{flag} = j \qquad (2.5.2)$$

The new flag is then set to the maximum of this flag and that derived from the data-base flags. The values currently used for $ERRLIM_{1-3}$ are 12.25, 25 and 36 for height, 8, 18, 20 for wind, and 2.25, 5.06, 7.56 for thickness.

For SATEMs the (thickness) limits are multiplied by 0.2, 0.6, 1.0, 1.0, 1.0, 0.9 and 0.7 respectively for the layers 1000/700 through to 30/10 hPa. AIREP reporting zero wind speed are rejected providing the first-guess wind speed is less than 5 m/s.

For SATOBs the (wind) limits above are multiplied by 0.1 except for low level winds ($p \geq 700$ hPa) and METEOSAT south of 20° S when they are multiplied by 0.2. Additionally, there is an asymmetric first-guess check, which is applied whenever the observed wind speed is more than 4 m/s slower than the first-guess. Then the limits are reduced further; for low level winds the limits are multiplied by 0.15; tropical, medium and high level winds by 0.07 and extratropical medium and high level winds by 0.075 - 0.00125 x $|v_{fg}|$.

2.5.3(c)   *Multi-level check*

An additional quality control check is applied following the first guess check, to all multi-level observations except TEMPSHIPS (*Shaw et al.* 1984). Each variable is examined in turn, taking account of the flags already set by either the first guess check or the preceding data-base checks. If four successive levels have flags ≥ 1, then these data are rejected. Furthermore, in case of geopotentials, all data at levels above the levels in question are also rejected. For satellite thicknesses, the complete profile is rejected. Data most commonly rejected by this test are TEMP geopotential data in the upper troposphere and stratosphere (*Lönnberg and Shaw*, 1985).

For SATEM the multi-level check works differently. The whole sounding is rejected whenever there is one layer or more with flag 3, two layers or more with flag 2 or at least 40% of the layers having flag 1.

2.5.3(d)   *Stability check*

A frequent problem with satellite temperature retrievals is the inability to represent correct lapse rate. Therefore, a stability check against the first-guess is carried out for SATEM. If the temperature difference between the two layers 1000/700 and 500/300 hPa differs more than ± 3.5 K from the first-guess, the whole profile is rejected. The limit is first-guess error dependent and thus larger in data sparse areas. A special reduction by up to 1 K is applied sinusoidally between 30° north and south.

2.5.3(e)   *Wind direction check*

In case of wind data, a wind direction check is carried out in addition to the standard first-guess check. If the observed wind direction differs by more than 60, 90 and 120 degrees from the first-guess wind direction, it is flagged 1, 2 or 3 respectively. This check is applied only to upper-air winds above 700 hPa and for wind speeds greater than 15 m/s.

2.5.3(f)   *Comparison with nearby observations*

In data dense areas some preliminary observation selection is performed before the actual analysis, to remove redundant information. This is done by combining observations of the same type within the same model box to form "super-observations". (See Section 2.6, Selection of Data, for details). The corners of a model box is defined by four neighbouring gridpoints on the Gaussian grid.

The "super-observation" creation is preceded by a full OI quality control (QC) of all observations to be averaged and observations of same type from all near neighbouring model boxes. Near neighbours are boxes with a common border. The "super-observation" is formed from those data, in the central model box, which passed the QC check. The data which contributed to the averaging are not used further in the analysis. As the average observation is constructed from data that have passed a proper QC, it is regarded as correct and cannot be rejected by any later QC check.

"Super-observations" are formed only among SYNOP and SATEM data and when at least 3 observations within the central box pass the QC test.

2.5.3(g)   *Comparison with analysis*

The mass and wind analysis program selects data, sets up and solves the analysis equations for "analysis volumes" (see Section 2.7 for details). The data checking is done by calculating the difference between each datum so far not checked and an analysis not using that datum $\left(\delta_k^o - \delta_k^i \right)$, and an estimated variance of this difference e^{io^2}. The expression (2.2.21) for e^{io^2} assumes that the correlations and error estimates used in the interpolation of δ^i are appropriate; it contains no allowance for errors due to the method itself or to

errors in the assumed statistics. To allow for this when checking data a term α is added to e^{io^2}. A datum is deemed to have failed the check if

$$\left(\delta_k^o - \delta_k^i\right)^2 > ALIMRJ_2 \left(e_k^{io^2} + \alpha\right) \tag{2.5.8}$$

α is an estimate of the analysis error when the amount of observations becomes infinite. In that situation the OI estimate of the analysis error e^i goes to 0. A reasonable approximation of the actual analysis error was obtained with the pre-1984 analysis system which did not select all lower tropospheric radiosonde data because of too high data density. The results from that study (Lönnberg and Shaw, 1985) suggested that the analysis error in lower troposphere is about 6-8 m for height with the increased analysis resolution. This value of α was set to 5 m.

$$\alpha = \frac{5m}{E_k^p (z, 1000 \ hPa)} \tag{2.5.9}$$

The denominator in (2.5.9) is the estimated forecast error of height at 1000 hPa at the observation point.

If more than one datum fails the worst failure is rejected and all other failures are retested not using it. Thus a flag in the range 0-3 is assigned to each datum:

$$\text{if } \left(\left(\delta_k^o - \delta_k^i\right)^2 > ALIMRJ_N \left(e_k^{io^2} + \alpha\right)\right) \text{ then flag} = N.$$

Values currently used for $ALIMRJ_{1,2,3}$ are 6, 9 and 12 except for SATEM when they are 4, 6, 8 and for SATOB which have 1, 1.5 and 2. For SATEM an additional multi-level check follows. If one or more layers within a slab (surface -100 hPa or 300-10 hPa) is rejected, all layers in the slab will be rejected.

2.5.3(h) *SHIP blacklist*

A dynamic list of bad SHIPs is maintained operationally. The flag set by the OI check (2.5.8) is recorded and a blacklisting procedure is executed for the next analysis cycle. The blacklisting is only applied to SHIPs with unambiguous call sign. A report is doubtful if either pressure or wind is flagged by the OI check (2.5.8). A SHIP is blacklisted if

(i)   It has reported at least 3 times during the last 48 hours

       and

(ii)   It has been flagged on the majority of occasions.

2.6   SELECTION OF DATA

2.6.1   Introduction

One of the most complex parts of an analysis system is the data selection. It should provide a representative set of observations for the analysis at a particular point or in the ECMWF scheme for all points in a volume with horizontal dimensions of the order of 1000 km square. Another important aspect of the data selection is the elimination of data redundancy. The upper bound of the analysis resolution is determined by the grid on which the analysis increments are evaluated. In practice the analysis resolution is considerably lower because of the filtering properties of the structure functions and the data density. Observations at higher density than the upper limit of analysis resolution are obviously redundant and can be compressed.

The data selection in the humidity analysis is organised in a similar way. The main difference is the vertical partitioning; only one tropospheric slab is used in the moisture analysis.

An example of the horizontal distribution of the analysis volumes, or boxes, for the North Atlantic and European regions, is shown in Fig.2.1. The selection of data advances in four steps.

(i)   Pre-analysis data organisation within one model row independent of the analysis.

(ii)   Reduction of data redundancy, i.e. "super-observation" formation

(iii)   The selection of the data for a specific analysis volume.

(iv)   Data selection for analysis evaluation.

2.6.2   Pre-analysis data organisation

The pre-analysis performs computationally inexpensive housekeeping tasks to compress the amount of data and to eliminate clearly erroneous observations before the main analysis. Most of the data quality control flags are set in the pre-analysis (see Section 2.5). Observations considered useless are discarded and redundant information is compressed by forming a "super-observation".

2.6.2(a)   *Discarding of observations*

One of the following reasons causes discarding of an observation before the data redundancy tests:

(i)   Position or time is flagged as suspicious by the quality control checks of the Reports Data Base.

(ii)   Observation time deviates more than three hours from analysis time.

(iii)   Observation format is unrecognisable.

(iv)   Level information is out of order for a single- level observation.

(v)   No data has been found in the observation.

A datum or report is discarded from further use if any of the following conditions is fulfilled:

SYNOP/SHIP:

(i)   Station has inappropriate reporting practice, i.e. it extrapolates pressure or height more than 800 m or is more than 100 hPa below model terrain.

(ii)   Land winds are not used if

        - | Latitude | >30° or

        - | Station height | >150 m or

        - | Model height | >150 m

(iii)   Discard all reports from same station, except the one closest to the analysis time. In case of moving platforms, search from 1°x1° box around the platform for a report with same unambiguous call sign. Call signs like SHIP, RIGG, PLAT, XXX are regarded as ambiguous.

AIREP: Same as for SHIPs, condition (iii)

DRIBU: Same as for SHIPs, condition (iii)

SATOB: Report over land and | latitude | >20°.

TEMP/PILOT:

(i)   Station has extrapolated pressure or height by more than 800 m.

(ii)   TEMP height is more than 100 hPa below model terrain

(iii)   Wind is more than 25 hPa below model terrain

(iv)   Land surface wind

(v)   Redundant data are removed from a pair of a TEMP and a PILOT, which are collocated and not more than 30 minutes apart, giving priority to the data in the TEMP.

SATEM:

(i)   Thicknesses over land with bottom level pressure > 100 hPa.

2.6.2(b)   *Reduction of data redundancy*

In data dense areas redundancy of observations is reduced by combining close observations of the same type. For details see Section 2.5.3(d). At present, "super-observations" are formed among SYNOPs and SATEMs if there are at least 3 obervations in a model box. The observation error of the "super-observation" is given by (2.2.15). However, the normalised observation error may not be less than 0.5.

2.6.2(c)   *Interface to main analysis*

The observations that passed the previous tests are eventually written to a global observation array which is kept in core during the rest of the mass and wind analysis.

A datum in an observation is discarded if

- Quality flag is 3 (incorrect), or at least 2 in case of non-standard level data from multi-level observations
- The normalised observation error ≥ 32
- The absolute value of the normalised observation deviation ≥ 16.

The observation is discarded in the case that due to these limits no data would be stored.

2.6.3 Data selection in main analysis

This part of the data selection is intended to collect a set of representative data to perform a multi-variate analysis for all gridpoints in the box and all levels in the slab. Simultaneously, the data set should not differ markedly from those of the neighbouring boxes or slabs in order to avoid discontinuities in the analysed values. The selection in the main analysis is divided in four different parts:

(i)   Construct box tree for data checking according to data density.

ii)   Selection of data for data checking, separately for each slab.

(iii)   Construct box tree for analysis evaluation.

(iv)   Selection of data for analysis evaluation, excluding rejected data, separately for each slab.

2.6.3(a)   *Definitions*

First, we define the areas/volumes involved in the data selection (see Fig. 2.3):

(i)   Model box:

Four neighbouring points on the model's Gaussian grid define a model box.

(ii)   Analysis box:

Here we distinguish between overlapping and non-overlapping analysis boxes. The non-overlapping boxes have no common area; only common boundaries. The overlapping boxes extend into the neighbouring boxes and are used in the increment evaluation stage.

(iii)   Minimum data selection area:

For every analysis box a minimum data selection area is defined. It covers the analysis box with near surrounding to give a representative data selection for every point within the analysis box.
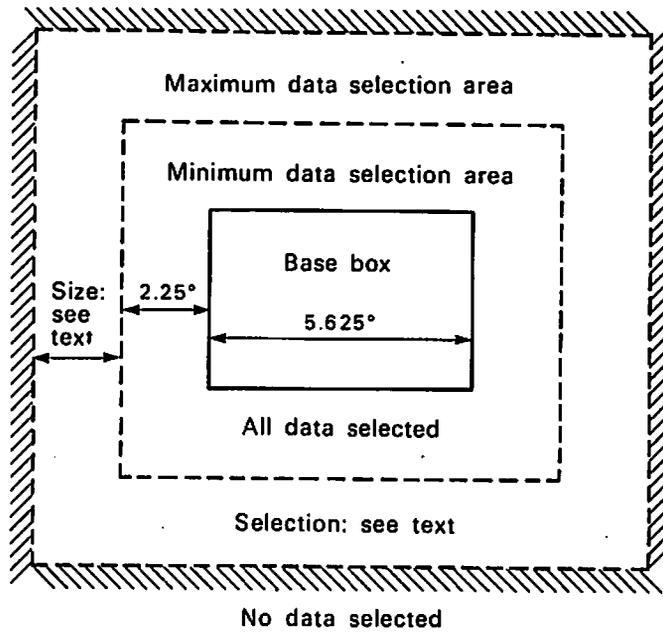
(iv)   Maximum data selection area:

A maximum data selection area is defined for every analysis box. Data outside this area are assumed to have no influence on the analysis and need not consequently to be selected.

2.6.3(b)   *Construction of box tree*

The construction of the box tree proceeds as follows:

DATA SELECTION

Maximum data selection area

Minimum data selection area

Base box

Size: see text

2.25°

5.625°

All data selected

Selection: see text

No data selected

BOX SUBDIVISION

>451 data

2 25°

Base box

>451 data
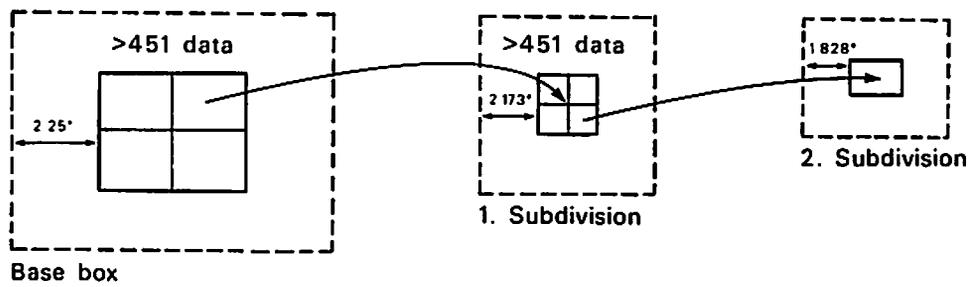
2 173°

1. Subdivision

1 828°

2. Subdivision

Fig. 2.3 Subregions associated with an analysis box, and the sampling sequence of the regions.

(i)   Base tree

The firsts step is to divide the globe into approximately equilateral base boxes. At present, there are 32 base box rows between the poles giving a meridional length of 5.625° for a base box. The minimum and maximum data selection areas are then assigned to each base box. The number of data within the minimum data selection area is counted for each vertical slab.

(ii)   Sub-boxes

If the number of data within the minimum data selection area exceeds the maximum allowed matrix size, at present 501, for any vertical slab, then the box is split in four sub-boxes of equal size in degrees latitude and longitude. For each new (and smaller) box, we define maximum and minimum data selection areas.

A further box split in four is made if the amount of data in the new minimum data selection area still exceeds the maximum matrix size in any slab.

2.6.3(c)   *Details of implementation*

(i)   Non-overlapping analysis box

Base box: 5.625° latitude and equivalent longitude

1. Subdivision: 2.8125° latitude

2. Subdivision: 1.40625° latitude

(ii)   Minimum data selection area

Each subdivision halves the minimum data selection area

Base box: 5.625° + 2 x 2.25° = 10.125° latitude

1. Subdivision: 2.8125° + 2 x 2.173 ~ 7.16° latitude

2. Subdivision: 1.40625 + 2 x 1.828 ~ 5.06° latitude

(iii)   Maximum data selection area.

The distance from the non-overlapping analysis box boundary to the outer limit of the maximum data selection area is given by

$$4^o \times \frac{L_c}{L_c^{min}} \cdot n + \frac{5.625}{2} \sqrt{2} \qquad\qquad (2.6.1)$$

where

L_c =   component length scale of forecast error (see Section 2.3.5(a)).

L_c^{min} =   global minimum of L_c

n =   1 in quality control

n = 2 in analysis evaluation

The reason for having a smaller search radius for the OI data check is discussed in *Cats*, 1981. The maximum selection distance (2.6.1) is independent of box subdivision.

The data selection proceeds as follows:

(i) Select all data within the minimum data selection area.

(ii) Continue outside minimum data selection area until 70% of maximum matrix size is reached according to rectangular distance from box centre. No data are selected beyond the maximum data selection limit.

The selection is done separately for each slab. The slabs are surface to 100 hPa and 300-10 hPa.

By permitting an overlap from one slab to the next in terms of data selected, one mitigates some of the effects that can arise from totally distinct selections for adjacent slabs. However in practice this overlapping may still be insufficient to guarantee smooth transitions, in terms of analysis increments, as one proceeds from one slab to the next. A serious consequence is found in the vertical profile of geopotential increments, where a discontinuity across a slab boundary transforms to an erratic profile of temperature increments. An ultimate solution to this problem is to avoid the vertical partitioning of the atmosphere. This is not feasible within the framework of the current system, given the constraints on matrix size and the size of the horizontal boxes in data rich regions.

The current approach, which mitigates the effects of the discontinuity, is to replace the analysis of geopotentials in the upper slabs by an analysis of thickness. By using the bottom slab to provide a reference level, one is effectively permitting the plentiful near-surface data to have an impact on the geopotential structure in the upper slabs without the data being explicitly used in those slabs. Such an approach has been incorporated in the current scheme (*Undén*, 1984).

2.6.3(d)   *Rejection of data*

The method of the spatial consistency check is described in Section 2.5. Only data which have flags 0 or 1 are used in the final analysis.

2.7   ORGANISATION OF THE COMPUTATION

2.7.1   Overview

Computationally the mass and wind analysis consists of three main stages:

(i) Preprocessing of observations, as described in Sections 2.4, 2.5 and 2.6.

(ii) Data checking by the statistical interpolation method, as described in Section 2.5.3(e).

(iii) Calculation of the changes (increments) to the first-guess, as described in Section 2.2.

As the matrix inversion is computationally expensive, the data selections for all gridpoints within an analysis volume are made to be identical (see Section 2.1) and hence the analysed values for several gridpoints are calculated simultaneously.

The globe is divided into rectangular areas (boxes) according to data density, as discussed in Sections 2.1 and 2.6. The atmosphere is divided into two layers in the vertical. For each such volume the appropriate data are selected and $\underline{B}^T \underline{M}^{-1}$, see (2.2.8), is solved. The analysis can then be projected on any grid by multiplication with $\underline{P}$. In the data checking phase the analysis is only evaluated at the locations of the observations in the volume currently being considered. In the analysis phase the increments are evaluated on model levels and standard pressure levels (*Undén*, 1984).

2.7.2 Horizontal overlapping of analysis increments

As the analysis might change dramatically between a box and its neighbour due to different data selections, analysis increments are also calculated for gridpoints in the neighbouring boxes based on the data selection of the current box. The final analysis increment at a point is formed as a weighted mean of the different estimates of the analysis at that point. This box "overlapping" extends to the minimum data selection boundary. The weight given to the increment at (x, y) from an analysis volume k

$$w_k = |x_{bk} - x| \cdot |y_{bk} - y| \tag{2.7.1}$$

where x_{bk} and y_{bk} are the nearest box boundaries. The final increment is a weighted average of the contributions from all influencing boxes.

2.7.3 Computation of model level increments

The analysis changes of mass and wind are evaluated at gridpoints in the model's Gaussian grid and at model hybrid levels instead of at standard pressure levels. The first step is to calculate the surface pressure increment. This is done hydrostatically by

$$\frac{g}{R_d} \frac{p_s^{fg}}{T_{2m}} \frac{\Delta z}{\left[1 + \left(\frac{1}{\varepsilon} - 1\right)q_{2m}\right]} \tag{2.7.2}$$

with the aid of the first guess of temperature (T_{2m}) and specific humidity (q_{2m}) at 2 m. p_s^{fg} is the first-guess surface pressure and Δz is the height increment at p_s^{fg}. $\varepsilon = R_d/R_v$.

By using the analysed surface pressure (p_s), the pressures at hybrid levels can be calculated. Then heights and wind increments are calculated at these pressures. The heights are evaluated at 'half' levels defined as

$$A_{k+1/2} + B_{k+1/2} \, p_s$$

except for the highest level ($A_{1/2}$, $B_{1/2}$ - 0) where the pressure is set to

$$p_{1/2} - \exp \{2 \ln[0.5(A_{1/2} + A_{11/2})] - \ln[A_{11/2}]\} \tag{2.7.3}$$

The wind levels are defined as

$$p_k - 0.5 \left[(A_{k+1/2} + B_{k+1/2} \, p_s) + (A_{k+11/2} + B_{k+11/2} \, p_s) \right] \tag{2.7.4}$$

i.e. the full model levels.

There is, however, a complication because the analysis can be done in two or more (at present 2) vertical slabs and the model levels will intersect slab boundaries. This means that a model level in one analysis box can either be in the bottom slab or in the middle slab or in between two slabs, all in the same analysis box depending on the orography. To accommodate this, each gridpoint has weights (being 0 or 1) assigned to it according to which slab it is in. Gridpoints in between two slabs (or the one closest if there are none in the layer) are overlapped. The analysis evaluations from the two slabs are simply averaged.

The decision about which slab a gridpoint belongs to is taken by using the first guess surface pressure, so that the p_s evaluation will be consistent with the model level height and wind evaluations.

The heights calculated at model 'half' levels are used to calculate virtual temperature increments at full model levels.

$$\Delta T_{v_k} - - \frac{g}{R \, \ln r} \left(\Delta z_{k+11/2} - \Delta z_{k+1/2} \right) \text{ where } r - \frac{(A_{k+11/2} + B_{k+11/2} \, p_s)}{(A_{k+1/2} + B_{k+1/2} \, p_s)}$$

However when the two height increments stem from different slabs which contain different data an inconsistency may arise. This can be quite severe and can cause very unrealistic temperatures, especially in thin model layers near the lower boundary. To overcome this problem an overlapping scheme has been designed and is described in Section 2.7.4.

The hybrid level increments of virtual temperature, winds and surface pressure are spectrally fitted and interpolated to the model's Gaussian grid. Then these fields are added to the first guess hybrid level Gaussian fields (after the first guess temperature has been converted to virtual temperature).

2.7.4 Analysis overlap in the vertical

The ECMWF analysis system is designed to use all the data in boxes with horizontal sides of about 500-1000 km in addition to some data from neighbouring boxes. There is a vertical division of the box into 2 slabs: 10-300 hPa and 100 hPa - surface. Due to the fact that different data have been used in the 2 slabs, the analysis at neighbouring levels can be quite inconsistent in some cases. In order to introduce some smoothing the analysis evaluations from adjacent slab are overlapped and averaged between 100 and 300 hPa. But still the temperature increments in the overlapped layer can be spurious. This could cause a problem over oceans when using sea level pressure from a SHIP and thickness data from SATEM in the lowest slab, and only thickness data in the higher slabs. When the evaluation of the analysis at model levels was tried, very unphysical temperature increments resulted when the lowest σ-layer intersected the slab boundary over high terrain. Therefore an overlap correction scheme for heights had to be designed for both model level evaluation and pressure level evaluation (*Undén*, 1984).

The analysis should produce heights that are such that the resulting thicknesses are always analysed thicknesses or a linear combination of analysed thicknesses from adjacent slabs.

To quantify the correction scheme let us consider the general case where more than one level may be overlapped from adjacent analysis slabs.

The height analysis from slab I is evaluated at levels $1,2,3...N-1$, N. The analysis in slab II is then evaluated at levels $N-k$, $N-k+1$, $N-k+2...M-1$, M, where N and M are the upper slab boundaries and $k \geq 0$ determines the degree of overlapping between the two slabs.

If we first consider the case when $k \geq 1$ (i.e. two or more levels overlap) the height analysis at level $N-k$ is 0.5 ($z_{N-k}^{II} + z_{N-k}^{I}$) where z^{I} and z^{II} denote the height analyses from the different slabs (i.e. using different data). The thickness of the layer below is then

$$\Delta z_{N-k} = 0.5 \left(z_{N-k}^{II} + z_{N-k}^{I} \right) - z_{N-k-1}^{I} \qquad (2.7.6)$$

This thickness is clearly spurious since different data have been used to analyse z_{N-k}^{II} and z_{N-k}^{I}. The aim of the overlapping correction scheme is to replace the thickness in (2.7.6) by an <u>analysed</u> thickness, namely

$$\Delta z_{N-k}^{I} = z_{N-k}^{I} - z_{N-k-1}^{I} \qquad (2.7.7)$$

This is accomplished by adding a correction term at level $N-k$ and all levels above

$$\Delta z_{N-k}^{I} = \Delta z_{N-k} = 0.5 \left(z_{N-k}^{I} - z_{N-k}^{II} \right) \qquad (2.7.8)$$

In other words the spurious thickness $\left(\Delta z_{N-k} - \Delta z'_{N-k}\right)$ is removed.

Now another problem arises in the layer above the lower slab (I). There the evaluated thickness would be

$$\Delta z_{N+1} = z^{II}_{N+1} - 0.5\left(z^{I}_N + z^{II}_N\right) \qquad (2.7.9)$$

The correct analysed thickness should be

$$\Delta z'_{N+1} = z^{II}_{N+1} - z^{II}_N \qquad (2.7.10)$$

and the correction term to be added to the height analysis at level $N+1$ and all levels above is

$$\Delta z'_{N+1} - \Delta z_{N+1} = 0.5\left(z^{I}_N - z^{II}_N\right) \qquad (2.7.11)$$

Thus for such an overlap there are two corrections to the height analyses - one at level $N-k$ and above [using (2.7.8)], and one at level $N+1$ and upwards [using (2.7.11)].

In the case of $k=0$, i.e. only one level is overlapped, the only difference is that the two corrections give the same value and it is added once at level N and twice at all levels above.

CHAPTER 3

Humidity Analysis

3.1 INTRODUCTION

The humidity analysis is designed on the same principle as the mass and wind analysis that the background field provided by the model forecast is generally quite accurate (*Lorenc and Tibaldi*, 1979). Its estimated error and the estimated observational errors of the various observation types are taken into account when determining the weights given to each observation (*Illari*, 1987). The interpolated value in the analysis is the deviation from the background field, so that if no datum disagrees with it the background field is unchanged. The analysis variable is relative humidity; the analysis is done for model levels between the surface and 250 hPa. Above 250 hPa the first-guess relative humidity is kept, except for the stratosphere.

The types of observation used in the humidity analysis, and their processing prior to the analysis, are described in Section 3.2. The analysis technique itself is described in Section 3.3.

3.2 OBSERVATIONS AND THEIR USE

Three types of observations - sondes, surface observations and estimates of precipitable water from satellites - are used in the analysis, all requiring some preprocessing of their basic information to render them useable in the analysis.

3.2.1 Radiosondes

Pressure, temperature T, and dew point T_D at both standard and special pressure levels are extracted from a radiosonde report. At each level the relative humidity w is calculated, as is its estimated rms observation error δw. The error of a radiosonde relative humidity measurement is assumed to be 15% (*Illari*, 1987). A dry observation (RH<20%) is also ascribed an error of 15% and a cold ($T<-40°C$) measurement is ascribed an error of 20%. Data up to 275 hPa are used in this procedure. No humidity data inside model mountains are used.

3.2.2 Surface observations

Surface observations, as well as providing direct humidity information by way of T and T_D, also report cloud amounts and types, from which humidity can be deduced. There have been several efforts to do this in the past (*Chisholm et al.*, 1968; *Atkins*, 1974; *Kaestner*, 1974; *Jonas*, 1976; *Tuller*, 1977); we have based our

system on a method used by NMC (*Chu and Parish*, 1977) and modified by *Pasch and Illari* (1985) and *Illari* (1986).

Each observation can provide up to four estimates of the relative humidity:

(i) T and T_D give w which is assigned to 2 metres. The tolerance for mismatch between station height and model orography is 10 hPa.

(ii)   Low, medium and high clouds estimate the humidity in three layers of the free troposphere. The values are assigned to the mean pressure of the layers:

$$P_{LOW} = \quad P. - 50 \text{ hPa} - \frac{1}{6} (P. - 50 \text{ hPa} - 300 \text{ hPa})$$

$$P_{MID} = \quad P. - 50 \text{ hPa} - \frac{1}{2} (P. - 50 \text{ hPa} - 300 \text{ hPa})$$

$$P_{HIGH} = \quad P. - 50 \text{ hPa} - \frac{5}{6} (P. - 50 \text{ hPa} - 300 \text{ hPa})$$

P. is the first-guess surface pressure and the thickness of the planetary boundary layer is assumed to be 50 hPa.

For all three layers the relative humidity estimate (and its associated error) as functions of cloud amount are:

$$RH_X = M_X - A_X \cos(\frac{\pi}{8} OKTAS_X) \tag{3.2.3}$$

$$RHER_X = 35 - \frac{5}{2} OKTAS_X \tag{3.2.4}$$

where $OKTAS_X$ is the cloud cover in eighths of a given layer X(=LOW,MID,HIGH) and M_X and A_X vary according to Table 3.1 (derived from *Chu and Parish*, 1977).

	M_x	A_x
HIGH	55	10
MIDDLE	60	15
LOW	75	15

Table 3.1   Coefficients for the estimation of relative humidity from cloud cover

The amount of cloud in each layer is derived from the cloud group in the SYNOP reports:

N   = total cloud amount
NN   = amount of cloud of the lowest reported type
NCL   = type of low clouds (0=no low clouds)
NCM   = type of middle clouds (0=no middle clouds)
NCH   = type of high clouds (0=no high clouds)

If N, NN or NCL has not been reported, no relative humidity estimate is created. Otherwise, the processing proceeds as follows:

(i)   Assign NN to the lowest layer that is reported to have clouds.

(ii)   If two types of clouds are reported assume that the clouds do not overlap and assign the cloud amounts:

        - upper reported cloud layer : N-NN
        - lower reported cloud layer : NN

        Three possibilities exist:

        - High and middle clouds (NCH>0, NCM>0, NCL=0)
        - High and low clouds (NCH>0, NCM=0, NCL>0)
        - Middle and low clouds (NCH=0, NCM>0, NCL>0)

(iii)   If three cloud layers reported (NCH>0, NCM>0 and NCL>0), use only NN to assign amount of low level clouds.

(iv)   CB clouds reported
        NN is assigned to all three cloud layers.

Pasch and Illari (1985) found that low cloud amounts are poor indicators of the atmospheric relative humidity. Only cloud values $\geq 7/8$ are used by the Synop bogusing (*Illari*, 1986).

3.2.3 Satellite precipitable water observations

Satellite soundings provide precipitable water content (PWC) for three tropospheric layers: surface - 700 hPa, 700-500 hPa and 500-300 hPa. From three values we derive PWC for five layers: surface - 850 hPa, 850-700 hPa, 700-500 hPa, 500-400 hPa and 400-300 hPa. The partitioning of the thick observation layers preserves the distribution of the PWC in the first-guess. Observations over land are not used since they have been seen to contain large biases. Also PWC data from reports without temperatures are discarded.

The moisture content of the background field is calculated by integrating

$$q = a + b\,p^{3.5}$$

(3.2.3)

in each model layer or parts thereof. a and b are determined from q at full model levels for each model layer. The power law formulation (3.2.3) has been shown to have the smallest global bias among several vertical interpolation techniques (*Mitchell*, 1985).

From collocation studies with radiosondes and comparisons against 6 hour forecasts, *Illari* (1987) found that the measurement error is about 10% RH. Due to large and noisy increments experienced over oceans the error is assumed to be 15% in the analysis. As the range of possible values for PWC is quite large, the effect of the rounding error in the report is included in the observation error calculation:

$$E_{obs} = [0.15^2 + E^2_{round}]^{1/2}$$

(3.2.4)

where

$$E_{round} = \frac{.5}{\dfrac{1}{g} \displaystyle\int_{p1}^{p2} q_s\, dp}$$

(3.2.5)

The numerator corresponds to the report accuracy of 0.5 mm water [kgm^{-2}] and the denominator is the amount of water the column would contain at saturation.

3.3   ANALYSIS TECHNIQUE

The algorithms employed by the humidity analysis are similar to those of the mass and wind analysis. The main differences to the mass and wind analysis are the following:

-       the analysis is univariate in relative humidity

- the specific humidity of the stratosphere is specified to $2.5.10^{-6}$. The "tropopause" is defined by the extremum of $\partial^2 T / \partial p^2$ between 70 and 500 hPa. The relative humidity at stratospheric levels may not exceed 90%

- the first-guess relative humidity at model levels between 250 hPa and the "tropopause" is preserved, if the "tropopause" pressure is less than 250 hPa. The specific humidity at these levels might still change as a result of temperature change in the analysis

- the humidity analysis is performed in one slab between surface and 250 hPa.

3.3.1 Forecast errors

At present, the prediction error is assumed to be independent of the accuracy of the previous analysis. The forecast error depends only on latitude:

- 10%   90°-30°N
- 15%   30°N-90°S

The prediction error correlation is assumed to have the form

$$\mu_{ik} = e^{-\frac{1}{2}(r_{ik}/r_o)^2}$$

(3.3.1)

where i, k refer to two locations and r_{ik} is their separation distance. r_o is currently assumed to be 300 km. The scale length and the error variances are in good agreement to the values found by *Illari* (1987).

3.3.2 "Super-observation" formation

Relative humidity "super-observation" can be formed among SYNOP observations within a model box. This process is similar to that of the mass and wind analysis (see Section 2.5.3(c)). The O/I algorithm gives an estimate of the observation error (2.2.15). However, this error estimate ignores small scale variations in the humidity field and may assign the "super-observation" an unreasonably low error. To avoid too high weight being given to a "super-observation", any normalised observation error less than 0.6 is modified to 0.6.

3.3.3   Quality control of data

The following quality control procedures are applied to humidity data:

(i)   Test of supersaturation

-     If the relative humidity value exceeds 120%, the data is rejected.

-     If the observed RH value is between 100% and 120%, it is changed to 100%.

(ii)   First guess check

A datum is rejected, if its normalised departure exceeds 5 standard deviations of the expected standard deviation of the difference between observation and first-guess.

(iii)   Multi-level check

-     Organise all levels in a report into analysis layers centred at standard pressure levels.

-     If the observation departure of at least one level in 4 consecutive analysis layers exceeds 3 standard deviations, then reject the whole report.

(iv)   Statistical interpolation check

A check against an independent analysis is also performed in the humidity analysis. The rejection limit is (cfr. 2.5.8):

$$(\delta_k^o - \delta_k^1) > 4^2 \cdot \varepsilon_k^{b^2}$$

3.3.4   Data selection

The same data selection algorithms as in the mass and wind analysis are applied for humidity. The selection parameters are as follows:

-     maximum matrix size: 501

-     maximum number of observations: 201

-     data checking/analysis evaluation: no overlap

-     minimum data selection area:

Base box: $5.625° + 2 \times 2.75° = 11.125°$ latitude

1. subdivision: $2.8125° + 2 \times 2.527° \sim 7.87°$ latitude

2. subdivision: $1.40625 + 2 \times 2.078° \sim 5.56°$ latitude

-     maximum data selection area:

analysis box + $2 \times 5°$ latitude

(or for base box $15.625°$ latitude)

3.4 TRANSFORMATION OF VIRTUAL TEMPERATURE AND RELATIVE HUMIDITY TO DRY TEMPERARURE AND SPECIFIC HUMIDITY

The first-guess contains the specific humidity

$$q_{fg} = \frac{\varepsilon e}{p-(1-\varepsilon)e} \tag{3.4.1}$$

where ε is R_d/R_v and e is the water vapour pressure.

The relative humidity in the first-guess is calculated from

$$w_{fg} = \frac{e}{e_s} = \frac{q_{fg}}{\varepsilon e_s(T_{fg})} (p-(1-\varepsilon)e_s) \tag{3.4.2}$$

where the water vapour saturation pressure is depending on the first-guess temperature according to (5.1.22).

Then the analysed relative humidity is formed by adding the analysis increments:

$$w = w_{fg} + \Delta w \tag{3.4.3}$$

From the mass and wind analysis, only the virtual temperature is known and it depends on the analysed specific humidity:

$$T_v = T\left(1+\left(\frac{1}{\varepsilon}-1\right)q\right) \tag{3.4.4}$$

To arrive at the analysed specific humidity and temperature, one needs to satisfy two simultaneous equations:

$$\begin{cases} q_{n+1} = \dfrac{w\varepsilon}{\dfrac{p}{e_s(T_n)}-(1-\varepsilon)} & (3.4.5) \\[3em] T_{n+1} = \dfrac{T_v}{1+\left(\dfrac{1}{\varepsilon}-1\right)q_{n+1}} & (3.4.6) \end{cases}$$

This is done by iteration. T_v is used as initial guess for T_n; q_{n+1} is computed from (3.4.5) and inserted in (3.4.6) which then gives a new T_{n+2} to be used to get q_{n+2} from (3.4.5). Convergence is fast but 11 iterations are done to ensure high accuracy.

CHAPTER 4

Analysis of surface fields

4.1 INTRODUCTION

In addition to the basic variables of mass, wind and humidity, the prediction model also requires some specification of certain surface parameters. The parameters which are analysed as part of the 6 hourly assimilation cycle are the sea surface temperature (SST) and snow depth.

4.2 SEA SURFACE TEMPERATURE (SST)

The analysis scheme for analysing the SST can be summarised as:

(a) Data input:

Global SST analysis from NMC Washington which is received via special telecommunication line. The data is specified on a regular $2^0 \times 2^0$ grid.

(b) Guess field:

ECMWF monthly climatological SST grid point values.

(c) Analysis method:

A successive correction method is used with the following characteristics:

- Increment calculation:

$$SST_x^i - \sum_{n=1}^{N} W_n \cdot D_n / \sum_{n=1}^{N} W_n$$

where, SST_x^i is the SST increment at the analysis point x, W_n is the weight given to the observation departure (observation minus climate) D_n at the observation point n.

- Weight function:

$$W_n - \left(R_{max}^2 - R_{xn}^2 \right) / \left(R_{max}^2 + R_{xn}^2 \right)$$

where, R_{max} is the influence radius and R_{xn} the distance between the points x and n.

- Scanning:

A three scan version is chosen:

scan no. 1 ; R_{max} = 700km

scan no. 2 ; R_{max} = 500km

scan no. 3 ; R_{max} = 300km

- Smoothing:

A 2-D smoother is applied on the increment field after the last scan.

- Quality control:

if at any point the observed value differs by more then 16°C from the interpolated climatological value the whole data input field is discarded.

- Resulting analysis:

$$SST_x^a - \left(SST_x^i + SST_x^c\right) - k \cdot MO_x; \quad k = 0.0065 \ K/m$$

where, SST_x^a and SST_x^c are the final SST analysis and climatological SST field. MO_x represents the height of the model's orography, which is non-zero over sea points due to its spectral fitting. Thus the final analysis is corrected for the model's orography assuming the constant lapse rate k. The SST analysis is a stepwise procedure. The first step consists of interpolating the monthly SST climatology from the ECMWF grid to the NMC grid (bilinear interpolation) and subtracting it from the NMC SST analysis, which results in the SST departures on the NMC grid. Then the SST analysis is performed for each sea point, resulting in the SST increments on the ECMWF grid. The next step is to interpolate the previously analysed SST increments back to the NMC grid in order to find the new SST departures which in turn become the input for the next SST analysis scan. The procedure is repeated for the required number of scans (three). The reason for using the SST increment field as guess input (from second scan onwards) is to preserve the small scale SST structures present in the climatological SST field. Special attention is paid to drawing the ice line. First, both the NMC SST analysis and the ECMWF SST climatology are set to -1.7°C (assumed freezing point) when they are below it. Thus, negative, zero and positive SST departures are possible in the vicinity of ice. They have an effect in the SST analysis is to melt, leave unchanged or freeze surrounding ice and water. In other words the SST analysis is specifying the ice edge. Also, this procedure enables a smooth ice-water transition and ensures that the climatological temperature values are kept over the permanent/semi-permanent ice areas.

4.3   SNOW DEPTH

The snow depth analysis scheme can be summarised in the following way. First, by using the snowfall observations and zero preliminary snowfall field, a snowfall analysis is performed. Then, by adding the snowfall analysis to the snow depth persistence analysis (previous analysis time), subtracting a possible snow melt and relaxing it towards the snow depth climate, a snow depth first guess field is created. Finally, by combining the snow depth observations and the snow depth first guess field, a snow depth analysis is carried out. The snow depth analysis scheme consists of three steps: (1) snowfall analysis, (2) construction of the snow depth preliminary field and (3) snow depth analysis. Through this three step procedure, the analysis is capable of using both the snowfall and snow depth observations, when available together. In the case of the snow depth observations not being available, the snow accumulation-melting cycle is simulated. The usage of the snow climate is twofold: firstly it ensures the stability of the scheme and secondly it gives a seasonal snow trend in areas without any snow observations.

4.3.1 Snowfall analysis

The snowfall analysis has the following characteristics:

(a)   Data input:

Snowfall observations are actually derived values from the precipitation and two metre temperature observations (available from SYNOP reports), based on the following assumption:

$$S_f^o = \begin{cases} P_r^o \; ; & T_{2m}^o \leq -2^oC \\ [1 - (T_{2m}^o + 2) / 4] \cdot P_r^o \; ; & -2^oC < T_{2m}^o < 2^oC \\ 0. \; ; & T_{2m}^o \geq 2^oC \end{cases}$$

where T_{2m}^o and P_r^o are the observed two metre temperature and precipitation, and S_f^o is the derived snowfall observation.

(b) Guess field:

No guess field is used.

(c) Analysis method:

A successive correction method is used with the following details:

- Snowfall analysis calculation:

$$S_{fx}^a = \sum_{n=1}^{N} W_n \cdot S_{fn}^o / \sum_{n=1}^{N} W_n$$

where, S_{fx}^a is the analysed snowfall value at the analysis point x, W_n is the weight given to the snowfall observation S_{fn}^o.

- Weight function:

The weighting of the observations is dependent on their horizontal and vertical displacement with respect to the analysis point:

$$W = H(R) \cdot V(dh)$$

with $H(R)$ and $V(dh)$ being the horizontal and vertical parts of the weight function:

$$H(R) = (R_{max}^2 - R_{xn}^2) / (R_{max}^2 + R_{xn}^2)$$

$$V(dh) = \begin{cases} 1. \; ; & dh > 0 \\ (H_{max}^2 - dh^2) / (H_{max}^2 + dh^2) \; ; & |dh| < H_{max}, \; dh < 0 \\ 0. \; ; & |dh| \geq H_{max}, \; dh < 0 \end{cases}$$

where R_{max} is the horizontal influence radius and R_{xn} the distance between points x and n, H_{max} is the height influence distance and dh the actual height difference (model minus station height).

- Scanning:

A one scan version is used:

scan no. 1 ; R_{max} = 250km ; H_{max} = 300m

- Quality control

In addition to the operational (report data base) quality control, the following checks are performed: firstly, when only one snowfall observation (within the influence radius) is available it is discarded; secondly, the total amount of analysed snowfall (or snow increase) at any grid point is checked against a limit L:

$$L = \begin{cases} 0. \; ; \; T_{2m}^{f} > 10^{b}C \\ 40.-4.\cdot T_{2m}^{f} \; ; \; T_{2m}^{f} < 10^{o}C \end{cases}$$

where L is the allowed snow increase in mm of equivalent water, and T_{2m}^{f} is the six hour forecast of two metre temperature.

4.3.2 Snow depth first guess field creation

The snow depth first guess field is constructed as:

$$S_{d}^{g} = [(1-a)\,(S_{f}^{a}+S_{d}^{p}) + a\cdot S_{d}^{c}] - M$$

where S_{d}^{g}, S_{d}^{p} and S_{d}^{c} are the first guess, persistence analysis and climatological snow depths, respectively, and S_{f}^{a} is the snowfall analysis. M is an empirical snow melting function and a is a relaxation coefficient:

$$M = \begin{cases} 0.025 \; T_{2m}^{\beta} \; mm \; of \; water \; /6hr \; ; \; T_{2m}^{f} > 0^{o}C \\ 0. \; ; \; T_{2m}^{f} \leq 0^{o}C \end{cases}$$

$$a = 0.02$$

4.3.3 Snow depth analysis

The details of the snow depth analysis are:

(a)   Data Input:

Snow depth observations (available from SYNOP reports) are used.

(b)   Guess Field:

Specially created field, as explained above in 4.3.2, is used.

(c)   Analysis method:

A successive correction method is used with the following details:

- Snow depth analysis increment calculation:

$$S_{dx}^i = \sum_{n=1}^{N} W_n \cdot D_n \Big/ \sum_{n=1}^{N} W_n + 1$$

where, S_{dx}^i is the snow depth increment at the point x, W_n is the weight given to the snow depth departure D_n.

- Weight function:

The weighting of the observations is done similarly as in case of snowfall analysis:

$$W = H(R) \cdot V(dh)$$

$$H(R) = (R_{max}^2 - R_{zn}^2) \,/\, (R_{max}^2 + R_{zn}^2)$$

$$V(dh) = \begin{cases} 1. \;; dh>0. \\ (H_{max}^2 - dh^2) \,/\, (H_{max}^2 + dh^2) \;; |dh|<H_{max}, \; dh<0. \\ 0. \;; |dh| \geq H_{max}, \; dh<0. \end{cases}$$

with symbols having the same meaning as before.

- Scanning:

One scan is applied:

scan no. 1 ; R_{max} = 250km ; H_{max} = 300m

- Quality control:

The first check applied is on the absolute values of snow depth observations; when the observed two metre temperature is below 10°C the acceptance limit is 140 cm, which is reduced to 70 cm if temperature is above 10°C. There is also first-guess check applied on the observation departure (observation minus first-guess value), for which the limit is 50 cm. Furthermore, as in case of snowfall analysis the total increase of snow is checked using the same expression for L (allowed snow increase). Also, the use of a single observation occurring within the influence radius is avoided. In case the following conditions are met: (1) more then half of the observations (within the influence circle) and (2) the first guess value, indicate no snow the snow depth increment is set to 0.

CHAPTER 5

Interpolation Methods

The mass and wind/humidity analysis requires the first-guess at the observation points. The forecast model is spectral, with data being expressed on a Gaussian grid for the physical parameterisations; and with a hybrid vertical coordinate. These differences require appropriate transformations between analysis and prediction model. All increments are evaluated directly on model levels and then added to the model first-guess. The transformations are described below. The transformations between grid point space and spectral space are done as in the forecast model (see Research Manual 2).

5.1   HYBRID TO PRESSURE TRANSFORMATION

The forecast model's vertical coordinate is described as 'hybrid' since it combines the characteristics of a sigma coordinate at lower levels with the characteristics of a pressure coordinate at higher levels. The hybrid coordinate is defined as

$$p_{k+1/2} = a_{k+1/2} + b_{k+1/2} \, p_s, \qquad 0 \le k \le NLEV$$

and $$\eta_{k+1/2} = \frac{a_{k+1/2}}{p_o} + b_{k+1/2}$$

where $a_{k+1/2}$, $b_{k+1/2}$ and p_o are constants.

The vertical interpolation from hybrid to pressure coordinates is, where possible, identical to the corresponding interpolation in the model post-processing (see Chapter 4 of Research Manual 2). Details of the vertical interpolation, together with any differences from the post-processing, are outlined below for each variable in turn.

5.1.1   Height

$$\eta_{k-\frac{1}{2}} \; \text{————} \; \phi_{k-\frac{1}{2}}$$

$$\text{--------------} \; T_k, q_k$$

$$\eta_{k+\frac{1}{2}} \; \text{————} \; \phi_{k+\frac{1}{2}}$$

The heights are computed by integrating the hydrostatic equation exactly using the ICAO temperature profile and only interpolate the difference between the model level heights and ICAO heights. The ICAO temperature profile is defined as

$$T_{ICAO} = T_o - \Lambda z$$

where T_o is 288 K, z the height above 1013.25 hPa and Λ is 0.0065 K/m.

Integration of the hydrostatic equation using this temperature profile gives T as a function of pressure:

$$T_{ICAO} = T_o \left(\frac{p}{p_o}\right)^\alpha \tag{5.1.4}$$

where $\alpha = \frac{\Lambda R}{g}$ and p_o 1013.25 hPa

Combining (5.1.3) and (5.1.4) gives the *ICAO* height profile as a function of pressure

$$z_{ICAO} = \frac{T_o}{\Lambda} - \frac{T_o}{\Lambda}\left(\frac{p}{p_o}\right)^\alpha \tag{5.1.5}$$

In particular, the *ICAO* height at the surface is:

$$z_{p_{sICAO}} = \frac{T_o}{\Lambda} - \frac{T_o}{\Lambda}\left(\frac{p_s}{p_o}\right)^\alpha \tag{5.1.6}$$

The *ICAO* heights refer to the 1013.25 hPa level. The heights above sea level using the *ICAO* temperature profile are then

$$z_{ICAO} = z_{p_{sICAO}} + z_s \tag{5.1.7}$$

where z_s is the height of the model orography $(z(p_s))$. Then the full height can be computed by adding the height difference between the integration of the hydrostatic equation using the full model temperature and integration using the *ICAO* temperature.

$$z_{k-1/2} = z_s + \frac{T_o}{\Lambda}\left(\frac{p_s}{p_o}\right)^\alpha + \sum_{NLEV}^{k} \frac{R_d}{g}\left[T_k\left(1+\left(\frac{1}{\epsilon}-1\right)q_k\right) - T_{ICAO}\right] \cdot \ell n \frac{p_{k+1/2}}{p_{k-1/2}} - \frac{T_o}{\Lambda}\left(\frac{p}{p_o}\right)^\alpha \tag{5.1.8}$$

for $1 < k \le NLEV$

with $\epsilon = R_d/R_v$ and q the specific humidity.

The first two terms are constant, the third, the difference term, is interpolated linearly in $\ell n(p)$ whereas the last term is computed analytically directly to the observation pressure p.

There is a stratosphere defined in the *ICAO* atmosphere. This is where the temperature has decreased to $T_{st} = 216.5$ K above which the temperature is kept constant. The pressure of the *ICAO* troposphere is from (5.1.4):

$$p_{trop} = p_o \left(\frac{T_{st}}{T_o}\right)^{\frac{1}{\alpha}} \tag{5.1.9}$$

The last term in (5.1.8), which represents the analytical integration of the hydrostatic equation with a constant temperature gradient, has to be integrated to the tropopause for pressures lower than p_{trop}. Above the tropopause one has to integrate using the constant temperature T_{st}. In the stratosphere the last term in (5.1.8) is replaced by:

$$-\frac{T_o}{\Lambda}\left(\frac{p_{trop}}{p_o}\right)^{\alpha} + \frac{R_d}{g}\,T_{st}\,\ell np_{trop} - \frac{R_d}{g}\,T_{st}\ell np$$

$$-\,T_{st}\left(\frac{R_d}{g}\,\ell np_{trop} - \frac{1}{\Lambda}\right) - \frac{R_d}{g}\,T_{st}\ell np \qquad (5.1.10)$$

For the top layer of the model $k=1$ in 5.1.8 and $\ell n\,\dfrac{p_{k+\frac{1}{2}}}{p_{k-\frac{1}{2}}}$ is replaced by $2\ell n2$.

$\left(\dfrac{p}{p_o}\right)^{\alpha}$ is calculated as $e^{\alpha(\ell np-\ell np_o)}$ for efficiency reasons.

ℓnp_k is defined as $\left(\dfrac{\partial}{\partial p}\,(p\,\ell np)\,-\,1\right)_k$

$-\,\dfrac{1}{\Delta p_k}\left(p_{k+\frac{1}{2}}\,\ell np_{k+\frac{1}{2}} - p_{k-\frac{1}{2}}\,\ell np_{k-\frac{1}{2}}\right) - 1$ to be consistent with the forecast model.

Above the second half level of the model ($k_{1\frac{1}{2}}$, $p_{1\frac{1}{2}} = 20hPa$) the linear interpolation has been found to be very inaccurate. Instead, for this layer a quadratic interpolation in ℓnp is employed, using the heights from the three highest half levels of the model

$$z(\ell np) = a + b\ell np + c(\ell np)^2 \qquad (5.1.11)$$

where a, b and c are constants determined so that (5.1.11) fits the heights at the three top levels ($k = \frac{1}{2}$, $1\frac{1}{2}$, $2\frac{1}{2}$). The interpolation formula then becomes

$$z(\ell np) = z_2 \quad + \quad \frac{(z_2 - z_1)\,(\ell np - \ell np_2)\,(\ell np - \ell np_3)}{(\ell np_2 - \ell np_1)\,(\ell np_1 - \ell np_3)}$$

$$- \quad \frac{(z_2 - z_3)\,(\ell np - \ell np_1)\,(\ell np - \ell np_2)}{(\ell np_2 - \ell np_3)\,(\ell np_1 - \ell np_3)} \qquad (5.1.12)$$

where the suffices 1, 2 and 3 refer to $k=\frac{1}{2}$, $1\frac{1}{2}$ and $2\frac{1}{2}$.

For $p > p_s$, the geopotential is calculated as follows:

(i) Find T_s, the surface temperature, assuming a constant lapse rate of $\beta = 6.5 \times 10^{-3}$ K/m:

$$T_s = T_{NLEV} + 6.5 \times 10^{-3} \times \frac{R_d}{g} T_{NLEV} \, \ell n \left(\frac{p_s}{p_{NLEV}} \right) \tag{5.1.13}$$

$\ell n \dfrac{p_s}{p_{NLEV}}$ is approximated by $\left(\dfrac{p_s}{p_{NLEV}} - 1 \right)$

(ii) Find T_0, the temperature at mean sea level, assuming the same lapse rate:

$$T_0 = T_s + 6.5 \times 10^{-3} \times \frac{\phi_s}{g}$$

(iii) Depending on the values of T_0 and T_s, the geopotential is calculated in three different ways:

a) if $T_0 \leq 290.5$

the hydrostatic equation is integrated with a constant lapse rate, $\beta = 6.5 \times 10^{-3}$ K/m, as above.

$$\phi = \phi_s - \frac{R_d T_s}{\alpha} \left(\left(\frac{p}{p_s} \right)^\alpha - 1 \right) \tag{5.1.15}$$

where $\alpha = \dfrac{\beta R_d}{g}$

If $\left(\dfrac{p}{p_s} \right)^\alpha = e^{\alpha \ell n \frac{p}{p_s}}$ is expanded in a Taylor series, (5.1.15) can be written

$$\phi = \phi_s - R_d T_s \, \ell n \frac{p}{p_s} \left(1 + \tfrac{1}{2}\alpha \ell n \frac{p}{p_s} + \frac{1}{6} \left(\alpha \ell n p \frac{p}{p_s} \right)^2 \right) \tag{5.1.16}$$

b) $T_0 > 290.5$ and $T_s > 290.5$

The lapse rate is reduced to zero.

$$\beta = 0 \rightarrow \alpha = 0 \tag{5.1.17}$$

T_s is reset to

$$T_s = 0.5(290.5 + T_s) \tag{5.1.18}$$

and the geopotential is calculated with the constant temperature T_s using (5.1.16).

c) $T_o > 290.5$ and $T_* \leq 290.5$

The lapse rate is reduced to

$$\beta = \frac{290.5 - T_*}{z_s} \rightarrow \alpha = \frac{R_d(290.5 - T_*)}{\phi_s} \qquad (5.1.19)$$

and the geopotential again calculated from (5.1.16).

The height is then obtained, using $h = \phi/g$ \qquad\qquad (5.1.20)

5.1.2   Horizontal wind

Linear interpolation in ℓnp is used to interpolate u and v to all analysis pressure levels, p, such that $p_{NLEV} \geq p \geq p_1$.

For $p < p_1$, the wind components are extrapolated linearly with respect to pressure, using the values at p_1 and p_2.

For $p > p_{NLEV}$, the wind components are taken to be constant with the value of the lowest level.

5.1.3   Humidity

(i)   Interpolate specific humidity, q, and saturation specific humidity, q_s, to the observation pressure from the nearest full model levels. Within the model layer, q and q_s are assumed to be linear in $p^{3.5}$ (*Mitchell*, 1985). Below the lowest full model level, q and q_s are assumed constant.

(ii)   The relative humidity, w, is calculated at the observation pressure using the model formulation:

$$w_k = \frac{q_k \times 100}{q_{s_k}}$$

where q_s, the saturation specific humidity, is defined as:

$$q_{s_k} = \frac{\dfrac{R_d}{R_v} \dfrac{e_s(T_k)}{p_k}}{1 - \left(\dfrac{R_v}{R_d} - 1\right) \dfrac{R_d}{R_v} \dfrac{e_s(T_k)}{p_k}} \qquad (5.1.21)$$

and $e_s(T)$, the saturation vapour pressure, is defined as

$$e_s(T_k) = c_1 \exp\left(\frac{c_3(T_k - T_o)}{T_k - c_4}\right) \tag{5.1.22}$$

with

$$T_o = 273.16$$

$$c_1 = 610.78$$

$$c_3 = \begin{cases} 17.269 & \text{for } T_k \geq T_o \\ 21.875 & \text{for } T_k < T_o \end{cases}$$

$$c_4 = \begin{cases} 35.86 & \text{for } T_k \geq T_o \\ 7.66 & \text{for } T_k < T_o \end{cases}$$

This formulation takes account of both the water and ice phases. Subscript k indicates observation k.

5.1.4   10 metre wind

The 10 metre wind is calculated using:

stable case

$$u_{10} = u_{NLEV} \left[\frac{z_{10}}{z_{NLEV}} + \frac{\sqrt{C_D}}{k} \left\{ \ell n \left(\frac{z_{10} + z_o}{z_o} \right) \frac{z_{10}}{z_{NLEV}} \ell n \left(\frac{z_{NLEV} + z_o}{z_o} \right) \right\} \right] \tag{5.1.23a}$$

unstable case

$$u_{10} = u_{NLEV} \left\{ 1 - \frac{\sqrt{C_D}}{k} \ell n \left[1 + \left(e^{k/\sqrt{c_D}-1} \right) * \frac{z_o (z_{NLEV} - z_{10})}{z_{NLEV}(z_{10} + z_o)} \right] \right\} \tag{5.1.23b}$$

where z_o = roughness length

z_{10} = 10 = height of 10 m surface

z_{NLEV} = height of lowest model level

i.e. $z_{NLEV} = T_{v_{NLEV}} * \frac{R_d}{g} * \ell n \left(\frac{P_{NLEV+\frac{1}{2}}}{P_{NLEV}} \right)$ \hfill (5.1.24)

C_D = drag coefficient for momentum

k = Karman constant

There are similar equations for v_{10}.

[In the post-processing, the roughness length z_o is dependent on the stability of the lowest model layer.]

5.1.5   2 metre temperature

The 2 metre temperature is calculated using:

Stable case

$$S_2 - S_s = [S_{NLEV} - S_s] * \left[\frac{z_2}{z_{NLEV}} + \frac{C_h}{k\sqrt{C_D}} \left\{ \ln\left(\frac{z_2+z_o}{z_o}\right) - \frac{z_2}{z_{NLEV}} \ln\left(\frac{z_{NLEV}+z_o}{z_o}\right) \right\} \right]$$

(5.1.25a)

Unstable case

$$S_2 - S_s = [S_{NLEV} - S_s] * \left\{ 1 - \frac{C-h}{k\sqrt{C_D}} \ln\left[1 + \left(e^{C k/H_s\sqrt{C_D}-1} \right) * \frac{z_o(z_{NLEV}-z_2)}{z_{NLEV}(z_2-z_o)} \right] \right\}$$

(5.1.25b)

with $S = C_p(q) \, T + gz$ so that

$$T_2 = \frac{S_2 - gz_2}{c_{pd} \left(1 + (\delta-1) \, q_{NLEV} \right)}$$

since q_2 is not available at this stage and where

z_o = roughness length

z_2 = 2 = height of 2 m surface.

z_{NLEV} = height of lowest model level, calculated using Eqn.(5.1.24).

C_D = drag coefficient for momentum

C_h = drag coefficient for heat

k = Karman constant

$\delta = c_{pv}/c_{pd}$

5.1.6   2 metre specific humidity

The 2 metre specific humidity is calculated using

$$q_2 = q_{NLEV} \left[\frac{q_{s_2}(T_2, P_2)}{q_{s_{NLEV}}(T_s, P_s)} \right]$$

(5.1.26)

with

$$p_2 = p_s \left[1 - \frac{2 \times g}{R_d \, T_2 \left(1 + (\frac{1}{e} - 1) \, q_{NLEV} \right)} \right]$$

and $e = R_d / R_v$

CHAPTER 6
Normal Mode Initialization

6.1   INTRODUCTION

Primitive equation models, unlike quasi-geostrophic models, generally admit high frequency gravity wave solutions, as well as the slower moving Rossby wave solutions. If the results of the analysis scheme are used directly as initial conditions for a forecast, subtle imbalances between the mass and wind fields will cause the forecast to be contaminated by spurious high-frequency gravity-wave oscillations of much larger amplitude than are observed in the real atmosphere. Although these oscillations tend to die away slowly due to various dissipation mechanisms in the model, they make the forecast noisy and they may be quite detrimental to the analysis cycle, in which the six-hour forecast is used as a first-guess field for the next analysis. The synoptic changes over the six-hour period may be swamped by spurious changes due to the oscillations, with the consequence that at the next analysis time, good data may be rejected as being too different from the first-guess field. For this reason, an initialization step is performed between the analysis and the forecast, with the object of eliminating the spurious oscillations.

The principle of the method is to express the analysed fields in terms of the normal modes of free oscillation of the model atmosphere, then to modify the coefficients of the fast moving gravity modes in such a way that their rate of change vanishes.

6.2   COMPUTATION OF THE NORMAL MODES

The first step is to compute the modes of free oscillation of the model atmosphere. For this purpose the model equations are linearized about a basic state at rest, with a temperature profile $\bar{T}(\eta)$ function of height only. The model equations can be written in matrix form:

$$\frac{\partial D}{\partial t} - f\xi + \beta\mu \nabla^2 P - R_D = 0$$

$$\frac{\partial \xi}{\partial t} + \beta V + fD - R_\xi = 0 \qquad\qquad (6.2.1)$$

$$\frac{\partial P}{\partial t} + \underline{B} D - R_P = 0$$

The terms on the right hand side contain all the nonlinear tendencies and are here set to zero. The vector notation is used in (6.2.1) to represent the values at all the model levels. The vertical structure matrix $\underline{B}$ is given in *Simmons and Strüfing* (1981, Eq.4.5). It depends on the basic state chosen and on the numerical

technique used in the vertical discretization. The auxiliary potential P is defined as $P - \bar{\phi} + \bar{RT} \; \ell np_s$. In the definition of the geopotential of the mean state $\bar{\phi}$ a mean surface pressure $\bar{p}_s$ is assumed.

In order to separate the vertical dependence from the horizontal in (6.2.1) the model variables $\underline{D}$, $\underline{\xi}$ and $\underline{P}$ are expressed in terms of the eigenvectors $\underline{\phi}_m$ of matrix $\underline{B}$. For example:

$$\underline{D} - \sum_{m=1}^{M} D_m \underline{\psi}_m \tag{6.2.2}$$

The equations obtained after substitution of 6.2.2 into 6.2.1 have the form of M independent systems of shallow-water equations with equivalent geopotential depth ϕ_m, equal to the eigenvalue corresponding to $\underline{\psi}_m$.

After performing the vertical separation, the M two-dimensional systems may be separated in the zonal direction by Fourier transforming the variables; thus we write e.g.

$$D_m \; (\lambda, \; \theta, \; t) - \sum_{k=0}^{N-1} D_{m,k} \; (\theta, \; t) \; \exp \; (ik\lambda) \tag{6.2.3}$$

If we now call $x_{m,k}$ the vector which contains $D_{m,k}$, $\xi_{m,k}$ and $P_{m,k}$ (scaled to be non-dimensional), the system of linear equations becomes formally:

$$\frac{dx_{m,k}}{dt} - i \underline{A}_{m,k} \; x_{m,k} \tag{6.2.4}$$

The matrix $\underline{A}_{m,k}$ is real and symmetric. Hence its eigenvectors are orthogonal. They form a set of horizontal normal modes which can be used to express x (dropping the indices m, k for simplicity of notation):

$$x - \sum_{l=1}^{3L} c_l \; \xi_l \tag{6.2.5}$$

In fact these modes naturally divide into two classes: symmetric and antisymmetric with respect to the equator. This property is used to reduce the dimension of the matrix $\underline{A}$ when finding its eigenvectors which are the normal modes required.

6.3 THE INITIALIZATION PROCESS

Using (6.2.5), the equation (6.2.4) can now be written

$$\frac{dc_l}{dt} = i \, v_l \, c_l \tag{6.3.1}$$

for each l, with v_l being the eigenvalues of $\underline{A}$.

Hence

$$x(t) = \sum_l c_l(0) \, \exp(i v_l t) \, \underline{\xi}_l \tag{6.3.2}$$

where the amplitudes $c_l(0)$ are determined by the values of D, ξ, P at t = 0. At least for the first few vertical modes (with large equivalent depths ϕ_m) there is a clear distinction between low-frequency Rossby wave solutions (small v_l) and high frequency gravity wave solutions (large v_l). Only solutions of the former type are observed in the atmosphere with significant amplitude.

If the real model equations were linear, it would be easy to ensure that high frequency gravity waves do not exist by simply reducing to zero the corresponding normal mode coefficient $c_l(0)$ of the analysis. But this method does not work for the full nonlinear model.

The equivalent of (6.3.1) for the nonlinear equations is

$$\frac{dc_l}{dt} = i \, v_l \, c_l + r_l(t) \tag{6.3.3}$$

The term r_l is the projection of the nonlinear terms of the model equations (computed by running one time step of the model) onto the normal modes. If we simply make $c_l = 0$ for $t = 0$, very soon this mode will reappear, forced by r_l. This was shown by *Williamson* (1976).

Machenhauer (1977) has proposed an iterative scheme for removing the gravity- mode oscillations by setting the initial time-derivatives of the gravity-mode coefficients to zero. From (6.3.3),

$$\left(\frac{dc_l}{dt}\right)_{t=0} = 0 \quad \text{if} \quad c_l(0) = -\frac{r_l(0)}{i v_l} \tag{6.3.4}$$

Since the nonlinear term $r_l(0)$ depends partly on the gravity-mode coefficients themselves, it is necessary to iterate the procedure; but for a barotropic model (or for the first few vertical modes of a multi-level model) the scheme converges rapidly, and two iterations are perfectly adequate.

In the current version of the analysis cycle we perform two iterations of *Machenhauer's* procedure, initializing just the first five vertical modes. (The higher internal modes have very low frequencies and thus do not contribute to the problem of spurious high-frequency oscillations). The nonlinear forcing terms are computed by running the model itelf for one timestep at each iteration.

Although in principle the non-linear forcing can include the "physics" package as well as the dynamics, in practice this leads to the immediate divergence of the iteration process. Following *Wergen* (1987), an estimate d_1 of the quasi-stationary part of the physical forcing is used, which is kept constant for all iterations. This estimate is computed by time-averaging the physical tendencies during a 2 hour forecast starting from an uninitialized analysis. Only those components which force inertia-gravity waves with periods longer than a certain cut-off period are retained, thus discarding less reliable small-scale structures. Operationally this cut-off period is 5 hours. In order to obtain only the stationary part of the physical forcing, the diurnal cycle is switched off during this 2 hour forecast.

The filter condition (6.3.4) now reads:

$$c_i(0) = - \frac{r_i(0) + d_i}{i v_i}$$

(6.3.5)

Since the initialisation condition (6.3.4) requires stationarity for the initialisation of inertia-gravity waves, it clearly mishandles the tidal component of the atmospheric circulation. It should be allowed to propagate westwards and therefore be excluded from the initialisation process. Again, following *Wergen* (1987), this is achieved by performing a time series analysis of the total dynamical and physical tendencies for the ten days preceding the actual analysis time. The westward propagating component with a 24 hour period for zonal wavenumber one and a 12 hour period for zonal wavenumber two are excluded from (6.3.4) for all five vertical modes and for the eight gravest meridional modes. With t_e being the tidal component of the tendencies, the initialisation condition becomes:

$$c_e(0) = - \frac{r_e(0) + d_e - t_e}{i v_e}$$

(6.3.6)

The steps of the initialization procedure can be summarized as follows:

1. Run model for 2 hours from the uninitialized analysis to compute time- averaged physical forcing without diurnal cycle.
2. Filter physical forcing field.
3. Run adiabatic model for one timestep to compute non-linear terms.
4. Compute new gravity mode coefficients according to (6.3.6)

5. Restore analysed surface pressure after first iteration.

6. As 3 but starting from results of first iteration step.

7. As 4 (second iteration).

CHAPTER 7

Monitoring of observation and analysis quality

7.1   USE OF ASSIMILATION STATISTICS

Operational data assimilation systems use short-range forecasts to provide the background field for the analysis. By comparing the background field to observations, we may infer the forecast error and its structure as well as the observation error characteristics (*Hollingsworth et al.*, 1986). Also, verification of the analysis against observations demonstrates the effectiveness of the analysis scheme to extract the relevant meteorological information from observations. Comparison of observations against initialised analyses quantifies the degree to which the analysed information can be retained by the forecast model.

A very important aspect of data assimilation is the monitoring of all observing systems using the assimilation system. Several studies to assess the quality of various observing systems have been made at ECMWF (*Delsol*, 1985, *Illari*, 1987, *Kelly*, 1985, *Lange*, 1985, *Hollingsworth and Lönnberg*, 1986, *Lönnberg and Hollingsworth*, 1986).

7.2   STATISTICS ARCHIVES

The collection of assimilation statistics started in January 1983 with radiosonde information and has now been extended to all data types. The archives contain the following information:

A.   observation header

      coordinates

      date and time

      observation type, code type

      station identifier

      station and instrument characteristics

B.   observation body (repeated for all levels)

      pressure(s)

      observed values (wind, height/thickness, temperature, dew point, humidity parameters)

      departure of observed values from first-guess, analysis and initialised analysis.

      quality control flags from

            Reports data base check

            first-guess check

            statistical interpolation check

REFERENCES

Atkins, M.J., 1974: The objective analysis of relative humidity. Tellus, 26, 663-571.

Cats, G.J., 1981: A method for solving a system of linear equations efficiently in order to optimise the analysis code: operational implementation. ECMWF Research Department Tech.Memo.No.33.

Cats, G.J., 1982: Construction of a vertical correlation matrix. ECMWF Res.Dept.Memo R2302/672.

Chisholm, D.A., J.T. Ball, K.W. Veigas and P.V. Luty, 1968: The diagnosis of upper-level humidity. J.Appl.Met., 7, 613-619.

Chu, R. and D. Parrish, 1977: Humidity analyses for operational prediction models at the National Meteorological Center. NOAA NMC Office Note 140.

Daley, R., 1985: The analysis of synoptic scale divergence by a statistical interpolation scheme. Mon.Wea.Rev., 113, 1066-1079.

Delsol, F., 1985: Monitoring the availability and the quality of observations at ECMWF. ECMWF Workshop on the Use and Quality Control of Meteorological Observations, 6-9 November 1984.

Eliassen, A., 1954: Provisional report on calculation of spatial covariance and autocorrelation of the pressure field. Inst.Weather and Climate Res.,Acad.Sci. Oslo, Rept. No.5.

Gandin, L.S., 1963: Objective analysis of meteorological fields. Translated from Russian by Israeli Program for Scientific Translations, 1965, 242pp.

Hollingsworth, A. and G.J. Cats, 1985: Estimates of round-off error in the inversion of positive definite matrices. ECMWF Research Department Tech.Memo.No.98.

Hollingsworth, A. and P. Lönnberg, 1986: The statistical structure of short-range forecast errors as determined from radiosonde data. Part I: the wind field. Tellus, 38A, 111-136.

Hollingsworth, A., D.B. Shaw, P. Lönnberg, L. Illari, K. Arpe and A.J. Simmons, 1986: Monitoring of observation and analysis quality by a data assimilation system. Mon.Wea.Rev., 114, 861-879.

Illari, L., 1986: The quality of ECMWF humidity analysis. ECMWF Workshop on High Resolution Analysis, 24-26 June 1985.

Illari, L., 1989: The quality of satellite pwc data and their impact on analyzed moisture fields. Tellus, 41A, 319-337.

Jonas, P.R., 1976: The use of surface synoptic data to estimate upper-level relative humidity over the sea. Met.Mag., 105, 44-56.

Kaestner, A., 1974: A procedure for objective analysis of relative humidity. Arch.Met.Geoph.Biokl., Ser.A., 23, 137-148.

Kelly, G.A., 1986: Statistical analysis of satellite sounding data and its application to the ECMWF analysis system. ECMWF workshop on High Resolution Data Assimilation, 24-26 June 1985.

Lange, A., 1985: The quality of TEMP data. ECMWF Workshop on the Use and Quality Control of Meteorological Observations, 6-9 November 1984.

Lönnberg, P. and A. Hollingsworth, 1986: The statistical structure of short-range forecast errors as determined from radiosonde data. Part II: the covariance of height and wind errors. Tellus, 38A, 137-161.

Lönnberg, P. and D. Shaw, 1985: Data selection and quality control in the EMWF analysis system. ECMWF Workshop on the Use and Quality Control of Meteorological Observations, 6-9 November 1984.

Lönnberg, P., 1988: High resolution analysis. ECMWF Res.Dept.Memo R2314/2258.

Lorenc, A.C., 1981: A global three-dimensional multivariate statistical interpolation scheme. Mon.Wea.Rev., 109, 701-721.

Lorenc, A.C. and S. Tibaldi, 1979: The treatment of humidity in ECMWF's data assimilation scheme. ECMWF Tech.Memo.No. 7.

Machenhauer, B., 1977: On the dynamics of gravity oscillations in a shallow water model, with application to normal mode initialization. Contributions to Atmospheric Physics, 50, 253-271.

Maher, J.V. and D.M. Lee, 1977: Upper air statistics. Australia. Surface to 5 mb 1957-1975. Meteorological Summary. Bureau of Meteorology, Australia.

Mitchell, K.E., 1985: A comparison of moisture variables in the vertical interpolations of a 4-D data assimilation system. Seventh Conference on Numerical Weather Prediction, AMS, June 17-20 1985, Montreal, Canada.

Norris, B., 1978: Quality control checks applied to observational data. ECMWF Tech.Note 23.1.

Oort, A.H. and E.M. Rasmussen, 1971: Atmospheric Circulation Statistic Professional Paper No.5. U.S. Dept. of Commerce/NOAA.

Pasch, R.J. and L. Illari, 1985: FGGE moisture analysis and assimilation in the ECMWF system. ECMWF Research Department Tech.Memo.No.110.

Rutherford, I., 1976: An operational 3-dimensional multivariate statistical objective analysis scheme. Proc.JOC Study Group Conference on Four- Dimensional Data Assimilation, Paris.

Schlatter, T.W., 1975: Some experiments with a multivariate statistical objective analysis scheme. Mon.Wea.Rev., 103, 246-257.

Schlatter, T.W., G.W. Branstator and L.G. Thiel, 1976: Testing a global multivariate statistical objective analysis scheme with observed data. Mon.Wea.Rev., 104, 765-783.

Shaw, D., P. Lönnberg and A. Hollingsworth, 1984: The 1984 revision of the ECMWF analysis system. ECMWF Tech.Memo.No.92.

Simmons, A.J. and R. Strüfing, 1981: An energy and angular momentum conserving finite difference scheme, hybrid coordinates and medium range weather prediction, ECMWF Tech.Rep.No.28.

Tuller, S.E., 1977: The relationship between precipitable water vapour and surface humidity in New Zealand. Arch.Met.Geoph.Biokl., Sea. A, 26, 197-212.

Undén, P., 1984: Evaluation of analysis increments at model levels. ECMWF Tech.Memo.No.94.

Undén, P., 1989: Tropical data assimilation and analysis of divergence. Mon.Wea.Rev., 117, 2495-2517.

Wergen, W., 1987: Diabatic nonlinear normal mode initialization for a spectral model with a hybrid vertical coordinate. ECMWF Tech.Rep.No.59, 83 pp.

Williamson, D.L., 1976: Normal mode initialization procedure applied to forecasts with the global shallow-water equations. Mon.Wea.Rev., 104, 195- 206.